International Journal of Aerospace Sciences 2013, 2(3): 71-91
DOI: 10.5923/j.aerospace.20130203.02

2 DOF H- Infinity Loop Shaping Robust Control for Rocket Attitude Stabilization

Swapnil Pramod Kanade*, Abraham T Mathew

Department of Electrical Engineering, National Institute of Technology, Calicut, 673601, Kerala

Abstract Robustness is the ability of a control system to maintain its performance and stability characteristics in the presence of all uncertainties. Attitude control of rocket is a benchmark problem in aerospace and missile guidance control because such a system is subjected to number of uncertainties like flight path change, mass variation, thrust variation, drag and so on. In this paper the robust control techniques for attitude control of rocket has been examined. The control problem consists of actuating of fin deflections by the autopilot which modifies angle of attack and sideslip angle while stabilizing the rocket rotational motion. In order to separate the uncertainties from nominal model, the uncertainties are expressed as diagonal structure in form of ULFT (Upper Linear Fractional Transforms) which avoids unnecessary conservation. Then 2 DOF H-∞ loop shaping technique is carried out for pitch rate control problem. This has been compared with H-∞ controller design technique. It has been observed that 2 DOF H-∞ loop shaping technique can provides good robust stability and performance. Extensive simulations have been carried out to evaluate system performance. The comparative results are included in this paper.

Keywords Robust Control, H-∞ Loop Shaping Control, Robust Performance

1. Introduction

Rockets differ from aircraft and spacecraft due to the rapidly time-varying parameters of their equations of motion, which often requires special guidance and control design strategies and short duration of flights. Furthermore, the fast response times required in both translation and rotation of rockets necessitate a much larger control loop bandwidth than that of either an aircraft or a spacecraft.

With the advancement in control theory, it is now possible to design control system using MIMO frame work. Also are new mathematical approaches that take into account for the modeling uncertainties, disturbance & measurement noise and render a robust controller. New methods have appeared in literature for attitude control of rocket. Forexample optimal control adaptive control , nuero- fuzzy control, robust control lyapunov based control design and genetic algorithm development. Adaptive technique assures high computation speed.

The rocket should be able to perform some maneuvers. This may include larger angle of attack, rapid rotational rate change, larger angular acceleration and wide variation in pressure and speed. This makes control problem challenging that requires guaranteeing robust stability and robust performance in presence of large parameter variation andun modelled dynamics with nonlinearities.

In 1981 Zames[1] brought H-∞ norm as a performance requirement. H-∞ control techniques developed by Doyle et al[2] ,Glover et al[3] not only offers the tradeoff between performance and control effort but also provides thecapabilities of accommodating the disturbance and parameter variation. Reichert[4] was the first to apply H-∞ control and to show how it advantages over classical control in autopilot design. Similar autopilot designs were considered byReichert Wise and Jackson. The autopilot robustness uncertain aerodynamic parameters are also examined by Wise.

From[11] we see that the H-∞ loop shaping controller was proposed by McFarlane and Glover in 1990. The systematic procedure was developed by Hyde in 1993. After that Limbeer,Kasenally and Perkinns extended it to 2 DOF loop shaping controller development and formulate standard H∞ optimization problem which allows to use model matching function in robust stabilization.

In this paper 2 DOF feedback H-∞ loop shaping techniques is applied for pitch rate control of rocket. Application to rocket model shows that closed loop system for pitch rate control is robust under structural natural frequency variation. In this paper aerodynamic data which is the function of Mach number 2.78 used for design purpose and the parameters are related to that described in[8]. The controller shouldguarantee stability for the model in addition to the performance specification that will be demanded.

Remaining part of the paper is organized as follows. Secti

* Corresponding author:
aprilswapnil@gmail.com (Swapnil Pramod Kanade)
Published online at http://journal.sapub.org/aerospace

on 2 describes about system modeling and equations of mot ion, linearization of model, uncertainty modeling. Section 3 includes 2 DOF loop shaping design details. Section 4 contains results, discussion & limitations of two approaches. Section 5 describes conclusion.

2. System Modeling

The model of rocket is first derived using 6 DOF custom variable mass blocks.

The six degrees of freedom consist of three translations, and three rotations, along and about the missile (X_b , Y_b, Z_b) axes. These motions are illustrated in Figure (1) the translations being *(u,v,w)* and rotation (*P,Q,R*) . Following Figure 1 shows complete 6 DOF representation of rocket

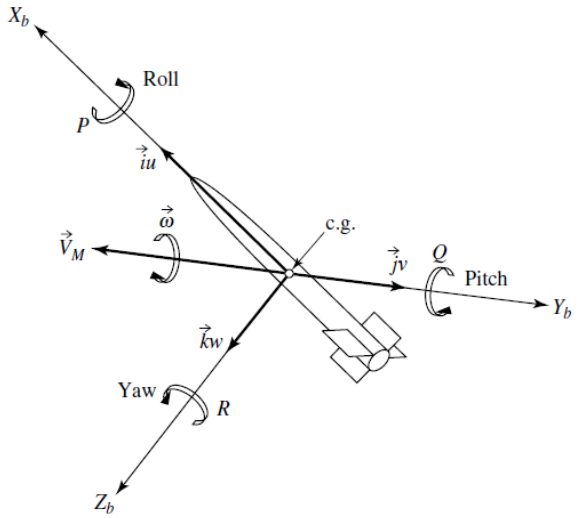

Figure 1. 6 DOF representation of rocket

In compact form, the translation and rotation of a rigid body may be expressed mathematically by the following equations.

Translation: $\sum F = ma$

Rotation: $\sum \tau = \frac{d}{dt}(r \times mv)$

2.1. Assumptions for Modeling of Rocket & Rocket Model Analysis

No model can be truly depicting its real system. So the model is only approximate representation of the behavior of the real system. The model for the rocket is derived based on following assumptions:[6],[9]

1. The rocket equations of motion are written in the body-axes coordinate frame.
2. A spherical Earth rotating at a constant angular velocity is assumed.
3. The vehicle aerodynamics are nonlinear.
4. The winds are defined with respect to the Earth.
5. An inverse-square gravitational law is used for the spherical Earth model.
6. The gradients of the low-frequency winds are small enough to be neglected.
7. A constant mass will be assumed, that is dm/dt =0
8. The aerodynamic forces and moments acting on the vehicle is assumed to be invariant with the position of rocket relative to the free stream velocity vector. Consequently the assumption greatly simplifies the equation of motion by eliminating the aerodynamic cross coupling terms between roll motion and pitch, yaw motion. In addition a different set of aerodynamic characteristics for pitch and yaw is not required.

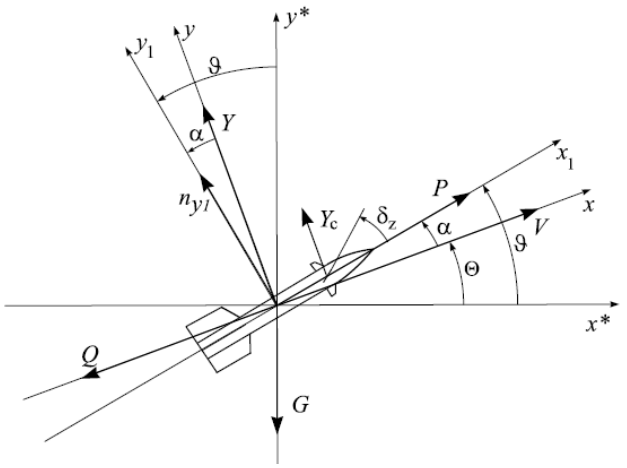

Figure 2. Pitch plane force diagram

In controller design only pitch perturbation motion is considered. In this case rocket attitude is characterized by pitch angle θ and flight path angle Θ or equivalently angle of attack α and θ. Due to rocket symmetry the yaw stabilization system is analogous to pitch stabilization system[7] . Hence equation of motion in pitch plane is considered. The followi ng Figure 2 shows complete free body diagram for pitch plane analysis with mathematical equations.[8-10].

In following Figure 2 reference frame notations used for writing equations of motion as the *x** -axis of the vehicle-ca rried vertical reference frame is directed to the North, the *y** -axis to the East. The x_1-axis of the body-fixed reference frame is directed towards to the nose of the rocket, the y_1-axis points to the top wing. The *x*-axis of the flight-path reference frame is aligned with the velocity vector V of the rocket and the *y*-axis lies in the plane $x_1\, y_1$.

1. Equations describing the motion of the mass centre

$$m\dot{V} = P\cos\alpha - Q - G\sin\Theta + F_x(t) \quad (1)$$

$$mV\dot{\Theta} = P\sin\alpha + Y - G\cos\Theta + F_y(t) \quad (2)$$

where

P = engine thrust.

Q = aerodynamic drag.

$F_x(t), F_y(t)$ = generalized disturbance forces in *x*, *y* direction.

m = mass of rocket

V = velocity of rocket

2. Equations, describing the rotational motion about the mass centre

$$\left.\begin{aligned} I_z\dot{\omega}_z &= M_z{}^f + M_z{}^d + M_z{}^c + M_z(t) \\ \dot{\theta} &= \omega_z \end{aligned}\right\} \quad (3)$$

wher $M_z{}^f$ = the rocket moments due to the angle of attack α

$M_z{}^d$ = the aerodynamic moments due to pitch rate ω_z

$M_z{}^c$ = the control moments due to fins deflection δ_z

$M_z(t)$ = generalized disturbance moments about corresponding axes.

$\dot{\theta}$ = pitch rate change

3 Equation giving the relationships between the angles α, θ, Θ

$$\alpha = \Theta - \theta \tag{4}$$

4 Equation giving the normal acceleration

$$n_y = -\frac{P\cos\alpha - Q}{G}\sin\alpha + \frac{P\sin\alpha + Y}{G}\cos\alpha \tag{5}$$

2.2. Linearization of Equations

In order to obtained a linear controller equations (1) – (5) are linearised about trim operating points $\Theta = \Theta^0$, $\theta = \theta^0, \alpha = \alpha^0, \omega_z = \omega^0{}_z, \delta_z = \delta^0{}_z$ under the assumptions that the variations $\Delta\Theta = \Theta - \Theta^0, \Delta\theta = \theta - \theta^0$, $\Delta\alpha = \alpha - \alpha^0, \Delta\omega_z = \omega_z - \omega^0{}_z, \Delta\delta_z = \delta_z - \delta^0{}_z$ are sufficiently small. In such a case it is fulfilled that $\sin\Delta\alpha \approx \Delta\alpha$, $\cos\alpha \approx 1$.

As a result, the linearised equations of the perturbed motion of the rocket take the form

$$\left.\begin{aligned}
&\dot{\Theta} = \tfrac{P+Y^\alpha}{mV}\alpha + \tfrac{Y^{\delta_z}}{mV}\delta_z + \tfrac{F_y(T)}{mV}\\
&\dot{\omega} = \frac{M^\alpha{}_z}{J_z}\alpha + \frac{M^{\omega_z}{}_z}{J_z}\omega_z + \frac{M^{\delta_z}{}_z}{J_z}\delta_z + \frac{M_z(t)}{J_z}\\
&\dot{\theta} = \omega_z\\
&n_y = \frac{Q+Y^\alpha}{G}\alpha + \frac{Y^{\delta_z}}{G}\delta_z\\
&\alpha = \theta - \Theta
\end{aligned}\right\} \tag{6}$$

where

$$Y^\alpha = c_y{}^\alpha qS\ ;\ Y^{\delta_z} = c^{\delta_z}{}_y qS\ ;\ M_z{}^\alpha = m_z{}^\alpha qSL\ ;$$
$$M^{\omega_z}{}_z = \frac{m^{\omega_z}{}_z qSL^2}{V}\ ;\ M^{\delta_z}{}_z = m^{\delta_z}{}_z\delta_z qSL$$

equations (6) can be represented as

$$\left.\begin{aligned}
&\dot{\Theta} = a_{\theta\theta}\alpha + a_{\theta\,\delta_z}\delta_z + \overline{F_y}(t)\\
&\ddot{\theta} = a_{\theta\,\dot{\theta}}\dot{\theta} + a_{\theta\theta}\alpha + a_{\theta\delta_z}\delta_z + \overline{M_z}(t)\\
&\alpha = \theta - \Theta\\
&n_y = a_{n_y\alpha}\alpha + a_{n_y\delta_z}\delta_z
\end{aligned}\right\} \tag{7}$$

where

$$a_{\theta\Theta} = \frac{P+Y^\alpha}{mV}\ ;\ a_{\theta\,\delta_z} = \frac{Y^{\delta_z}}{mV}\ ;\ a_{\theta\dot{\theta}} = \frac{M^{\omega_z}{}_z}{J_z}\ ;$$
$$a_{\theta\theta} = \frac{M^\alpha{}_z}{J_z}\ ;\ a_{\theta\delta_z} = \frac{M^{\delta_z}{}_z}{J_z}\ ;\ a_{n_y\alpha} = \frac{Q+Y^\alpha}{G}\ ;$$
$$a_{n_y\delta_z} = \frac{Y^{\delta_z}}{G}$$

In (7) we used the notation

$$\overline{F_y}(t) = \tfrac{F_y(t)}{mV} \text{ and } \overline{M_z}(t) = \tfrac{M_z(t)}{J}$$

Equations (7) are extended by the equation describing the rotation of the fins

$$\ddot{\delta_z} + 2\xi_{\delta_z}\omega_{\delta_z}\dot{\delta_z} + \omega_{\delta_z}{}^2\delta_z = \omega_{\delta_z}{}^2\delta_z{}^0 \tag{8}$$

Where $\delta_z{}^0$ is the desired angle of fins deflection (the servo actuator reference); ω_{δ_z} is the natural frequency and ξ_{δ_z} is the damping coefficient of servo actuator. The set of equations (7) and (8) describes the perturbed rocket longitu dinal motion. The coefficients in the motion equations are to be determined for the nominal (unperturbed) rocket motion. Nominal values of the parameters are assumed in the absence of disturbance forces and moments.

The unperturbed longitudinal motion is described by the equations .

$$\left.\begin{aligned}
&mV^* = P\cos\alpha^* - Q^* - mg_0\sin\Theta^*\\
&mV^*\dot{\Theta} = P\sin\alpha^* + Y^* - mg_0\cos\Theta^*\\
&\dot{H} = V^*\sin\Theta^*\\
&\dot{m} = -\mu\\
&\text{where}\\
&\alpha^* = \theta^* - \Theta^*\\
&\delta_z{}^* = -\frac{m_z{}^\alpha}{m^{\delta_z}{}_z}\alpha^*\\
&Q^* = c_x qS + c^{\delta_z}{}_x|\delta_z{}^*|qS\\
&Y^* = c^\alpha{}_y\alpha^* qS + c_y{}^{\delta_z}\delta_z{}^* qS\\
&q = \frac{\rho v^{*2}}{2}\ ;\ \rho = \rho(H)\\
&c_x = c_x(M)\ ;\ c^\alpha{}_y = c^\alpha{}_y(M)\ ;\ c_y{}^{\delta_z} = c_y{}^{\delta_z}(M)\\
&M = \frac{V^*}{a^*}\ ;\ a^* = a^*(H)\\
&m_z{}^\alpha = \frac{(c_x + c^\alpha{}_y)(x_G - x_C)}{L}\ ;\ m^{\delta_z}{}_z = \frac{c^{\delta_z}{}_y(x_G - x_R)}{L}\\
&\theta^* = \theta^*(t)
\end{aligned}\right\} \tag{9}$$

In these equations, $\theta^*(t)$ is the desired time program for changing the pitch angle of the vehicle.

2.3. Nominal Model and Stability of Model

A nominal system model has been obtained using the parameters given in the Table 1. The model is described in form of

$$\dot{x} = Ax(t) + Bu(t)$$
$$y = Cx(t) + Du(t)$$

Here $x(t) \in R^{m\times 2}$ is the state vector $u(t) \in R^{m\times 1}$ is the input vector $y(t) \in R^{p\times 1}$ is the output vector.

$$A = 1\times 10^4\begin{bmatrix} -0.0001 & 0.0001 & 0 & 0\\ -0.1217 & -0.0003 & 0 & 0.0286\\ 0 & 0 & 0.0212 & -2.2500\\ 0 & 0 & 0.0001 & 0\end{bmatrix}$$

$$B = \begin{bmatrix} 0\\ 0\\ 22900\\ 0\end{bmatrix}$$

$$C = [59.1024 \quad 0 \quad 0 \quad 28.7188]$$

$$D = [0]$$

For matrix A, the Eigen values $-2 \pm j\,34.87$ corresponds to stable mode and this pair explains system slow dynamics behavior. The pair $-106 \pm j\,106.13$ gives the unstable mode and explains about system fast dynamics.

Controllability index is 4. And hence system is fully cont rollable. The observability index is 4 and hence system is

fully observable. It is require to design $u(t)$ given by

$$u(t) = -Kx(t)$$

This will give a robust performance.

Table 1. System parameters

Symbol	Rocket Parameter	Value
L	Length of rocket	4.2 m
d	Rocket diameter	0.168 m
m	Initial rocket mass	96 kg
S_a	Engine nozzle output section area	0.0204 m^2
P_0	engine thrust at the sea level	740g N
μ	propellant consumption per second	0.7 kg/s
J_x	initial rocket moment of inertia about x axis	14.21 × 10 ^{2} kg M^2
J_y	initial rocket moment of inertia about y axis	7.64 kg M^2
J_z	initial rocket moment of inertia about z axis	7.64 kg M^2
X_G	initial rocket mass centre coordinate	1.7 m
X_C	initial rocket pressure centre coordinate	1.0 m
x_R	fins rotation axis coordinate	0.5 m
ω_n	natural frequency of the servo-actuator	236 Hz
ξ	servo-actuator damping	0.707
t_f	duration of the active stage of the flight	25 s
S	Reference area	0.094 m^2

2.4. Uncertainty Modeling

Separation of different uncertain parameters in different parts of model and combining into one block and forming ULFT is basic principle of uncertainty modeling[12]. For above rocket model main variation of coefficients of perturbed motion happens in aerodynamic coefficients $c_x, c^{\alpha}{}_y, m^{\alpha}{}_z, m_z{}^{\omega_z}$ and these are the function of mach number[7]. For above model 7 coefficients are considered as uncertainty given in equation (7). The uncertainty block Δ of all coefficients of variation is diagonal matrix of size 7×7. Complete ULFT model is shown in Figure 3

$$\Delta = diag(\delta_i)$$

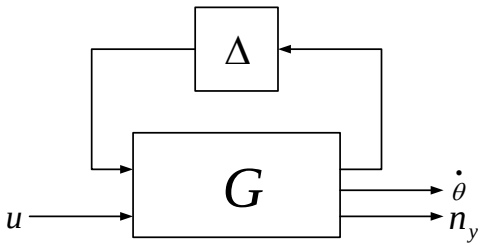

Figure 3. ULFT representation of model

3. H-∞ Loop Shaping Design

The loop-shaping design procedure described is based on H ∞ robust stabilization combined with classical loop shaping, as proposed by McFarlane and Glover 1992[5].

The open-loop plant is augmented by pre and post-compensators to give a desired shape to the singular values of the open-loop frequency response. Then the resulting shaped plant is robustly stabilized with respect to co prime factor uncertainty using H-∞ optimization. The H-∞ can make a balance between robustness, performance and stability of closed loop system.

3.1. Robust Stabilization Against Normalized Coprime Factor Perturbations[11]

To the normal system G constitutes left coprime factorization $G = M^{-1}N$. Considering its uncertainty a perturbed model as shown in Figure 4 can be described by

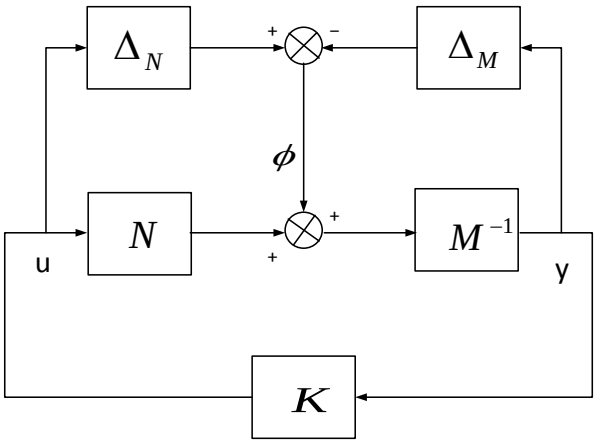

Figure 4. Normalized coprime factor uncertainty description

$$G = (M + \Delta M)^{-1}(N + \Delta N) \quad (10)$$

where ΔM *and* ΔN are unknown but stable transfer functions that represent uncertainty in nominal plant model.

The design objective of robust control is to make normal model G and family of perturbed plant stable. The family of perturbed plant is defined by

$$G = \{(M + \Delta M)^{-1}(N + \Delta N) : \|\Delta M, \Delta N\|_{\infty} < \varepsilon\} \quad (11)$$

where ε is stability margin. Using small gain theorem the feedback system is robustly stable if *(G,K)* is internally stable and

$$\left\| \begin{matrix} K(I - GK)^{-1}M^{-1} \\ (I - GK)^{-1}M^{-1} \end{matrix} \right\|_{\infty} \leq \frac{1}{\varepsilon} \quad (12)$$

In order to maximize the stability margin it needed to minimize the $\gamma = \frac{1}{\varepsilon}$

$$\gamma = \left\| \begin{bmatrix} K \\ I \end{bmatrix} (I - GK)^{-1}M^{-1} \right\|_{\infty} \quad (13)$$

Here γ is the H-∞ norm from ϕ to $\begin{pmatrix} u \\ y \end{pmatrix}$ and $(I - GK)^{-1}$ is the sensitivity function for this positive feedback arrangement. The lowest achievable value of γ and corresponding stability margin ε are given as

$$\gamma_{min} = \varepsilon_{max}{}^{-1} = \left\{1 - \|[N \;\; M]\|_H{}^2\right\}^{-0.5} = (1 + \rho(X\,Z))^{0.5} \quad (14)$$

where $\|.\|_H$ denotes the Hankel norm of system ρ denotes the spectral radius, and for minimal state space realization of G, Z is unique positive definite solution to algebraic Riccati equation

$$(A - BS^{-1}D^TC)Z + Z(A - BS^{-1}D^TC)^T - ZC^TR^{-1}CZ + BB^TS^{-1} = 0 \quad (15)$$

where

$$R = I + DD^T \ , S = I + D^T D$$

X is unique positive definite solution to algebraic Riccati equation

$$(A - BS^{-1}D^T C)^T X + X(A - BS^{-1}D^T C) - XB^T S^{-1} BX + C^T R^{-1} C = 0 \quad (16)$$

A controller which guarantees that

$$\left\| \begin{matrix} K(I - GK)^{-1} M^{-1} \\ (I - GK)^{-1} M^{-1} \end{matrix} \right\|_\infty \leq \gamma$$

for specified $\gamma > \gamma_{min}$ is given by

$$K = \begin{bmatrix} A + BF + \gamma^2 (L^T)^{-1} ZC^T (C + DF) & \gamma^2 (L^T)^{-1} ZC^T \\ B^T X & -D^T \end{bmatrix} \quad (17)$$

where

$$F = -S^{-1}(D^T C + B^T X) \quad (18)$$

$$L = (1 - \gamma^2) I + X \quad (19)$$

3.2. Two Degree of Freedom Controllers[10],[11]

In Doyle et al. and Limebeer et al.[5] a two degrees-of-freedom extension of the Glover-McFarlane procedure was proposed to enhance the model matching properties of the closed-loop . With this the feedback part of the controller is designed to meet robust stability and disturbance rejection requirements in a manner similar to the one degree-of-freedom loop-shaping design procedure except that only a pre-compensator weight W is used. It is assumed that the measured outputs and the outputs to be controlled are the same although this assumption can be removed as shown later. An additional pre filter part of the controller is then introduced to force the response of the closed-loop system to follow that of a specified model M called as reference model.

3.2.1. Scheme of 2 DOF Control

2 DOF H∞ loop shaping control is a robust control technique where the time domain specification can be incorporated in the design. The controllers designed by this approach are feed-forward pre-filter and feed- back controllers. The feed - forward pre-filter controller (K_1)is adopted to control the time domain response of the closed loop system, and the feed-back controller is designed for achieving the desired robust stability and the disturbance rejection requirement [10]. In this technique, only a pre compensator weight function (W_1) and reference model (M_{ref}) is needed to be specified. The shaped plant (G_s) is formulated as the normalized co prime factor which separates the nominal plant into normalized nominator & denominator (N_s,M_s) respectively.

The design problem is to find out stabilizing controller $K = [\, K_1 \, K_2]$ for shaped plant $G_s = GW_1$ with normalized coprime factorization $G_s = M^{-1}{}_s N_s$ which minimizes the H∞ norm of the transfer function between the signals $[r^T \ \phi^T]^T$ and $[u_s{}^T \ y^T \ e^T]^T$ as defined in Figure 5. Here ρ is a scalar value specified by the designer to assign the degree of significance of the time domain specification.

The control signal u_s to the shaped plant is given by

$$u_s = [K_1 \quad K2] \begin{bmatrix} \beta \\ y \end{bmatrix} \quad (20)$$

where K_1 is a pre filter and K_2 is a feedback controller , β is scaled reference and y is measured output. The purpose of pre filter is to ensure that

$$\left\| (I - G_s K_2)^{-1} G_s K_1 - M_{ref} \right\|_\infty \leq \gamma \rho^{-2} \quad (21)$$

From Figure 5 we have

$$\begin{bmatrix} u_s \\ y \\ e \end{bmatrix} = \begin{bmatrix} \rho(I - K_2 G_s)^{-1} K_1 & K_2 (I - G_s K_2)^{-1} M^{-1}{}_s \\ \rho(I - G_s K_2)^{-1} G_s K_1 & (I - G_s K_2)^{-1} M^{-1}{}_s \\ \rho^2 [(I - G_s K_2)^{-1} G_s K_1 - M_{ref}] & \rho(I - G_s K_2)^{-1} M^{-1}{}_s \end{bmatrix} \begin{bmatrix} r \\ \phi \end{bmatrix} \quad (22)$$

Here ρ is a scalar value specified by the designer to assign the degree of significance of the time domain specification[11].

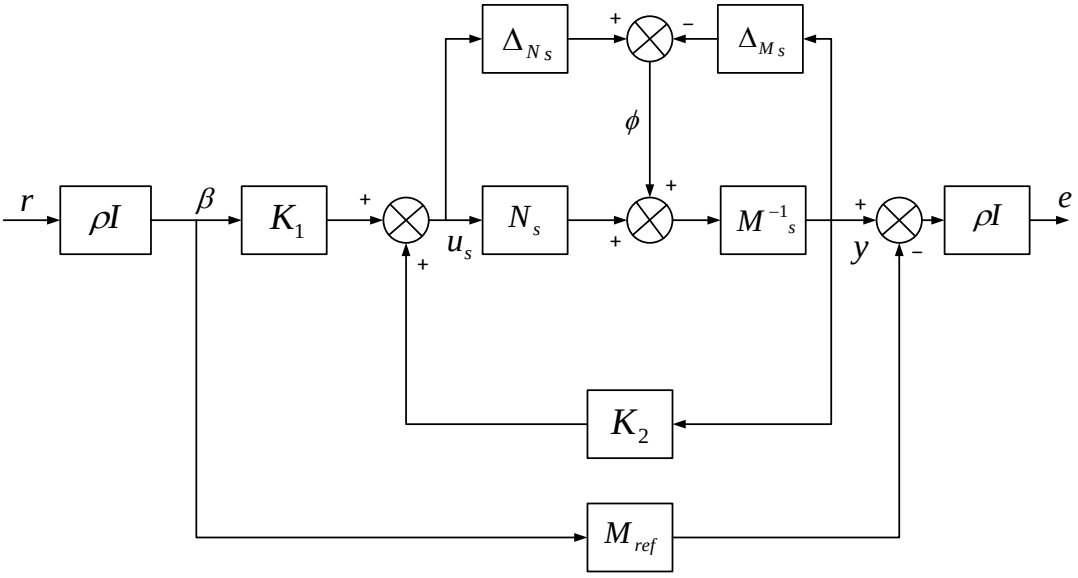

Figure 5. 2 DOF H-∞ loop shaping design

To put the 2 DOF design problem into the standard control configuration, we can define a generalized plant P by

$$\begin{bmatrix} u_s \\ y \\ e \\ \beta \\ y \end{bmatrix} = \begin{bmatrix} P_{11} & P_{12} \\ P_{21} & P_{22} \end{bmatrix} \begin{bmatrix} r \\ \phi \\ u_s \end{bmatrix} \quad (23)$$

$$\begin{bmatrix} u_s \\ y \\ e \\ \beta \\ y \end{bmatrix} = \begin{bmatrix} 0 & 0 & I \\ 0 & M^{-1}{}_s & G_s \\ -\rho^2 M_{ref} & \rho M^{-1}{}_s & \rho G_s \\ \rho I & 0 & 0 \\ 0 & M^{-1}{}_s & G_s \end{bmatrix} \begin{bmatrix} r \\ \phi \\ u_s \end{bmatrix} \quad (24)$$

Further if the shaped plant G_s and desired stable closed loop transfer function M_{ref} have the following state space realizations.

$$G_s = \begin{bmatrix} A_s & B_s \\ C_s & D_s \end{bmatrix} \quad (25)$$

$$M_{ref} = \begin{bmatrix} A_r & B_r \\ C_r & D_r \end{bmatrix} \quad (26)$$

Then P may be realized by

$$P = \begin{bmatrix} A_s & 0 & 0 & (B_s D_s{}^T + Z_s C_s{}^T) R_s{}^{-0.5} & B_s \\ 0 & A_r & B_r & 0 & 0 \\ 0 & 0 & 0 & 0 & I \\ C_s & 0 & 0 & R_s{}^{0.5} & D_s \\ \rho C_s & -\rho^2 C_r & -\rho^2 D_r & \rho R_s{}^{0.5} & \rho D_s \\ 0 & 0 & \rho I & 0 & 0 \\ C_s & 0 & 0 & R_s{}^{0.5} & D_s \end{bmatrix} \quad (27)$$

And used in standard H ∞ algorithm to synthesize controller K. note that R_s and Z_s are the unique positive definite solution to the generalized Riccati equation (15).

3.3. Design Procedure

The procedure to design 2 DOF H-∞ loop shaping controller as follows[11]:

1. Specify the pre-compensator weighting function (W_1) for achieving the desired open loop shape.

2. Specify M_{ref} which is the desired closed loop transfer function for time domain specifications and select ρ which is a scalar value between 0 and 1. If the designer selects $\rho = 0$, the 2DOF H-∞ loop shaping control becomes the 1DOF H-∞ loop shaping control.

3. Find optimal stability margin ε_{opt} by solving following equation

$$\gamma_{opt} = \varepsilon_{\text{opt}}{}^{-1}$$

$$= \left\| \begin{bmatrix} \rho(I - K_{2\infty} G_s)^{-1} K_{1\infty} & K_{2\infty}(I - G_s K_{2\infty})^{-1} M^{-1}{}_s \\ \rho(I - G_s K_{2\infty})^{-1} G_s K_{1\infty} & (I - G_s K_{2\infty})^{-1} M^{-1}{}_s \\ \rho^2[(I - G_s K_{2\infty})^{-1} G_s K_{1\infty} - M_{ref}] & \rho(I - G_s K_{2\infty})^{-1} M^{-1}{}_s \end{bmatrix} \right\|_\infty$$

4. Select the stability margin and then synthesize controllers $(K_{1\infty}, K_{2\infty})$ that satisfy

$$\|T_{zw}\|_\infty = \left\| \begin{bmatrix} \rho(I - K_{2\infty} G_s)^{-1} K_{1\infty} & K_{2\infty}(I - G_s K_{2\infty})^{-1} M^{-1}{}_s \\ \rho(I - G_s K_{2\infty})^{-1} G_s K_{1\infty} & (I - G_s K_{2\infty})^{-1} M^{-1}{}_s \\ \rho^2[(I - G_s K_{2\infty})^{-1} G_s K_{1\infty} - M_{ref}] & \rho(I - G_s K_{2\infty})^{-1} M^{-1}{}_s \end{bmatrix} \right\|_\infty$$

The elements (1,1) and (2,1) help to limit actuator usage, elements (2,2) and (1,2) are associated with robust stability optimization, (3,1) is used to model matching and element (3,2) is linked to the robust performance of the loop.

5. W_i is a scalar vector which is given by

$$W_i = \left[W_0 \left(-G_s(0) K_2(0) \right)^{-1} G_s(0) K_1(0) \right]^{-1} M_{ref}(0)$$

Where

$$W_o = \begin{bmatrix} 1 & 0 & 0 & 0 \\ 0 & 1 & 0 & 0 \\ 0 & 0 & 1 & 0 \end{bmatrix}$$

6. Final the feed forward pre filter and feedback controller $(K_1 \text{ and } K_2)$ can be determined by following equation

$$K_1 = W_1 K_{1\infty} W_i$$

$$K_2 = W_1 K_{2\infty}$$

The schematic diagram of controller is given in following Figure 6.

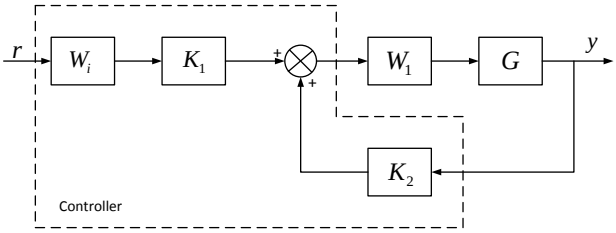

Figure 6. 2 DOF H-∞ loop shaping controller diagram

4. Simulation Results and Comparison of H-∞ Controller and H-∞ Loop Shaping Controller Design and Analysis

4.1. H-∞ Controller Design and Analysis

In our study the rocket parameters are selected from Table 1. Figure 7 shows generalized structure of H-∞ controller[13].

To design H-∞ controller, select the weight functions in such way that controller order will be equal to total number of system states plus weight function[14]. Basic requirement of weight function is to tune the controller[14].

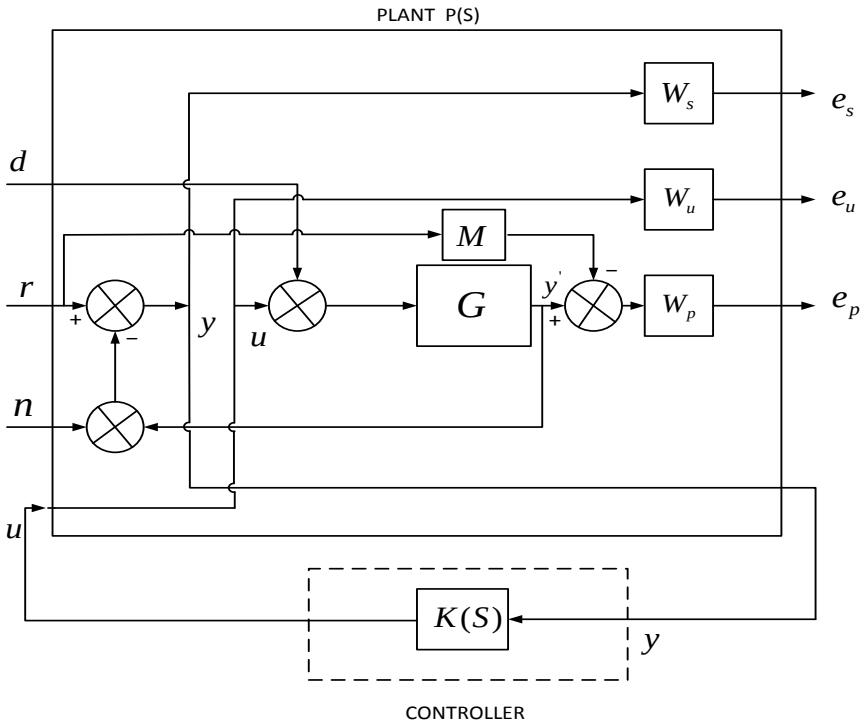

Figure 7. H-∞ generalized feedback control system

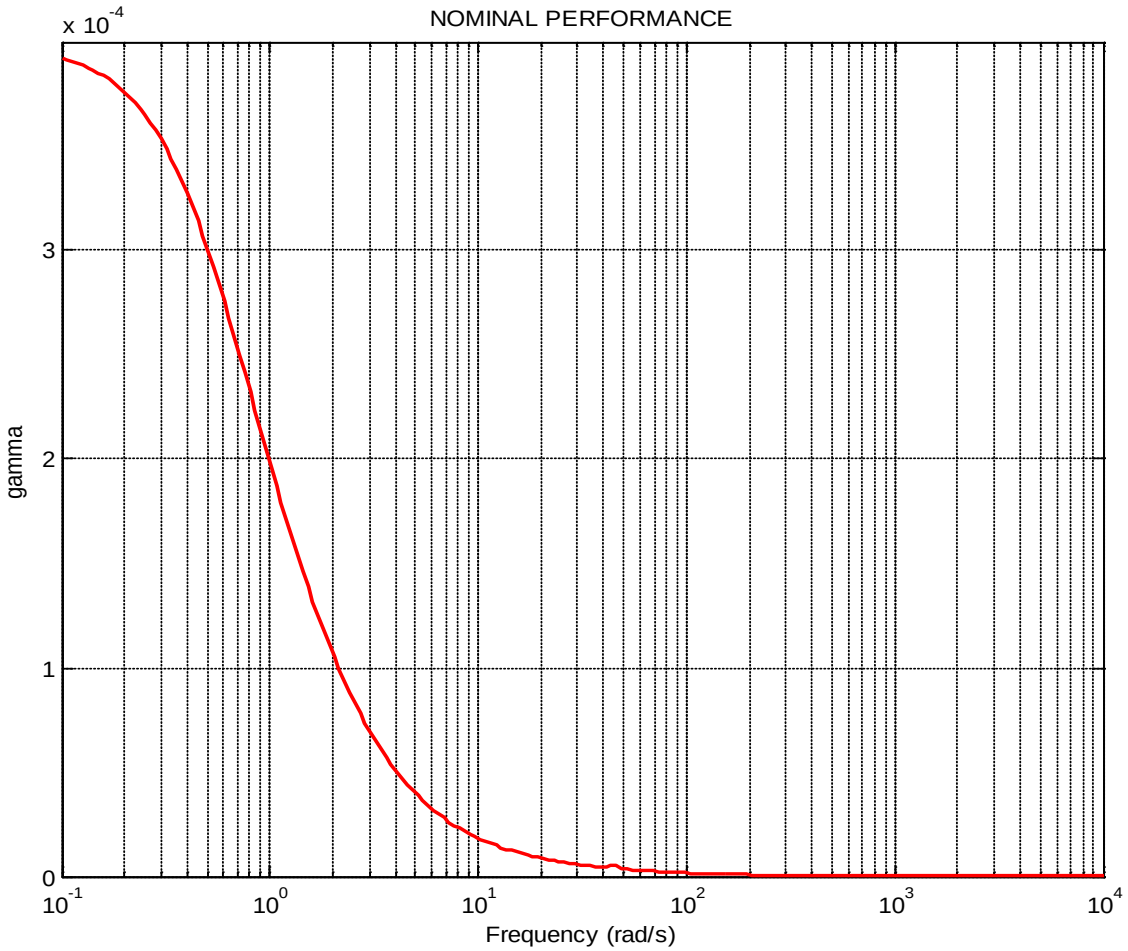

Figure 8. Nominal performance for H-∞ controller

The sensitivity weight function is selected as

$$W_s(s)^{-1} = 0.14\left(\frac{s^2+7s+2}{s^2+4s+9}\right)$$

Similarly complimentary sensitivity function is selected as

$$W_p(s)^{-1} = 0.6\left(\frac{s^2+4s+8}{s^2+10s+10}\right)$$

The tracking performance weight function W_s is aimed at minimizing low frequency tracking error and the robustness weighting function W_p is to reject high frequency multiplicative uncertainties[14]. In addition the control energy weight function is selected as

$$W_u(s)^{-1} = 0.3\left(\frac{s^2+4s+6}{s^2+7s+9}\right)$$

The objective is to avoid actuator operating at high frequencies which lead to saturation[16] . The model matching function is the ideal model to be matched by designed closed loop system which can be selected as[16]

$$M = \frac{1}{0.0256s^2+0.96s+1}$$

The actuator noise weight function chosen as

$$W_n = 0.95\times10^{-5}\left(\frac{0.17s+1}{0.0001s+1}\right)$$

With above data H-∞ controller is designed. The γ value obtained is 0.1509 which satisfies small gain theorem[12]. The nominal performance is analyzed and it is 0.00039808 as shown in Figure 8. The frequency response of structured singular values for the case of robust stability is shown in Figure 9. The maximum value of μ is 0.47663 which means that stability of closed loop system is preserved under all perturbations that satisfy $\|\Delta\|_\infty < \frac{1}{0.47663}$ [12] .The frequency response of μ for the case of robust performance analysis is given in Figure 10. The peak value of μ is 1.22245 which shows that robust performance has not been achieved.

Figure 11 shows the transient response of closed loop system with designed H-∞ controller for step signal with magnitude $r = \pm 5$ which corresponds to change in normal acceleration. The overshoot is 22.74% and settling time is 2.84 sec. The fins deflection obtained is 0.1881 rad. (11.78°) as shown in Figure 12. The pitch rate variation obtained is 0.1232 (rad/sec) shown in Figure 13 .

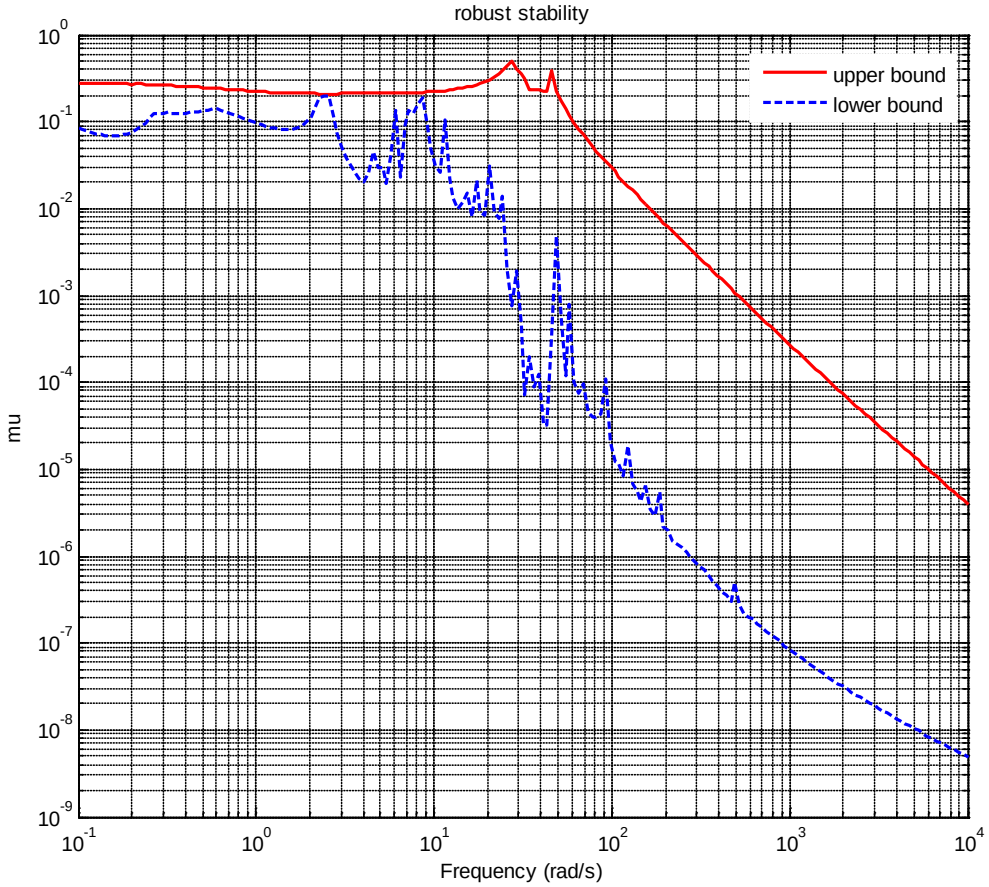

Figure 9. μ- Robust stability for H-∞ controller

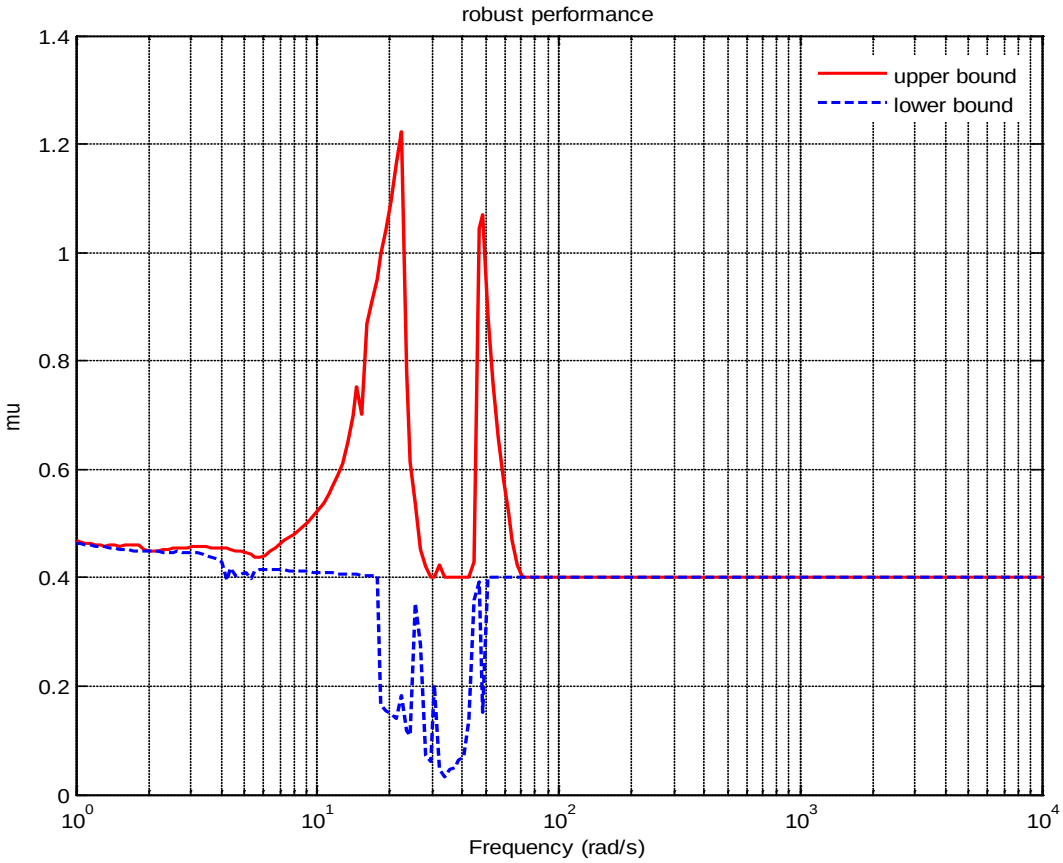

Figure 10. Robust performance for H-∞ controller

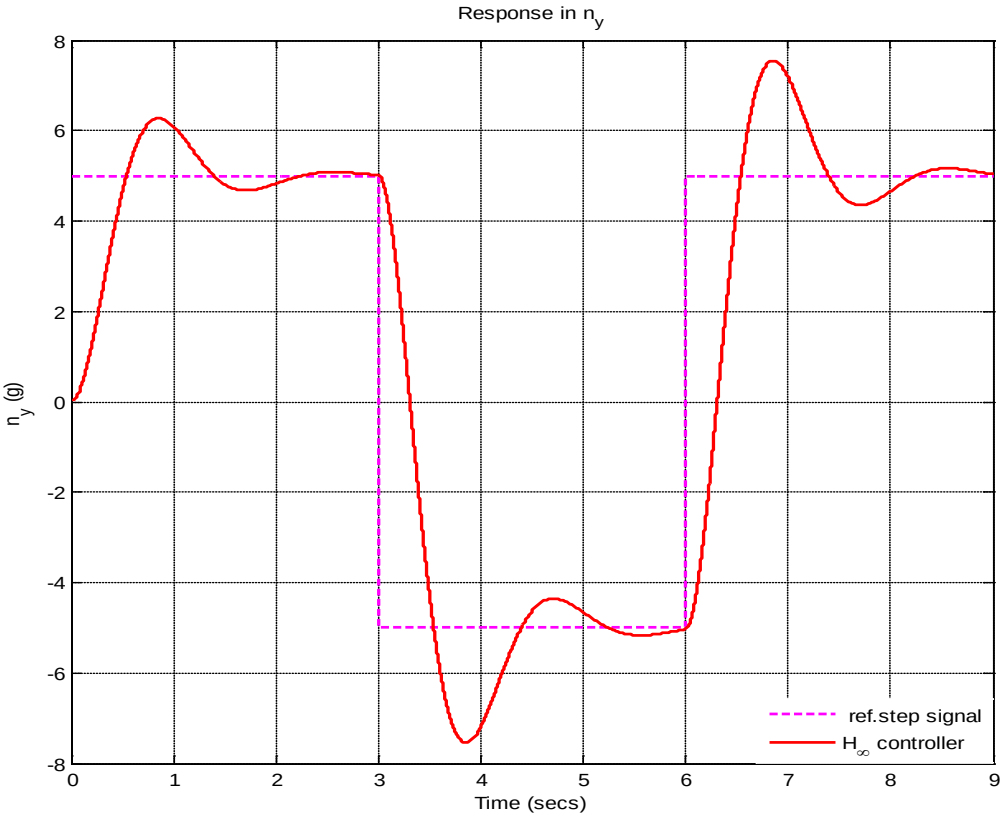

Figure 11. Acceleration response for H-∞ controller

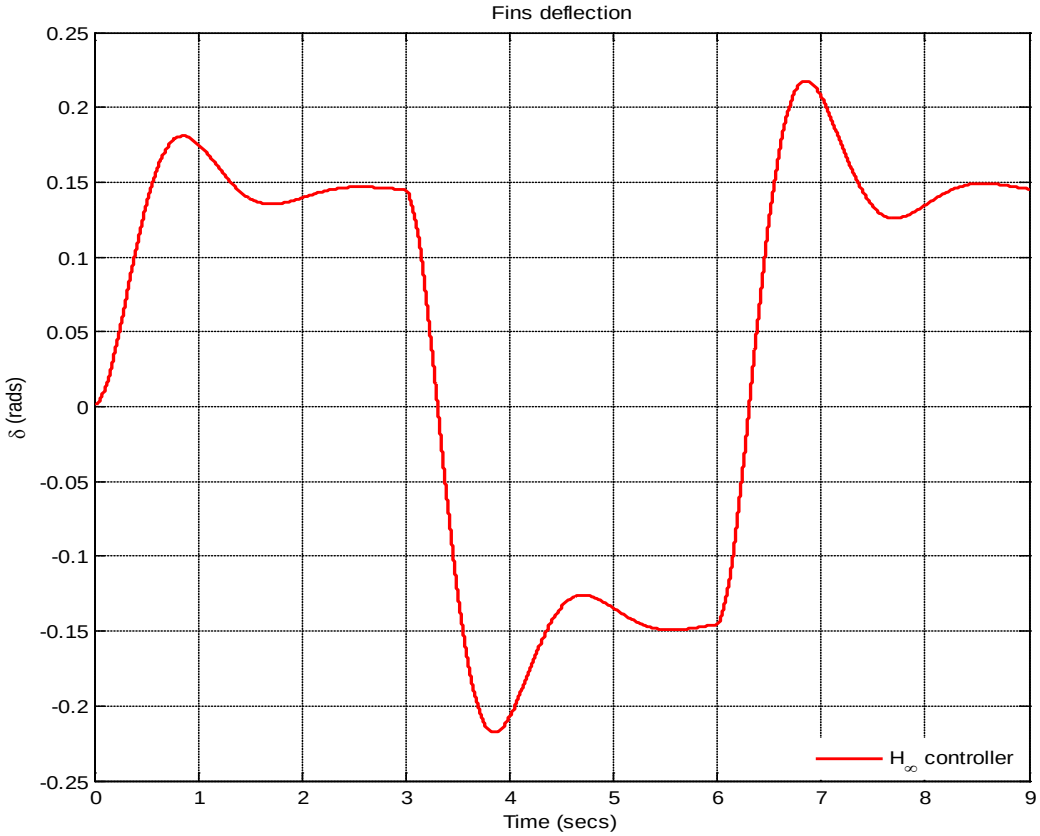

Figure 12. Fins deflection response for H-∞ controller

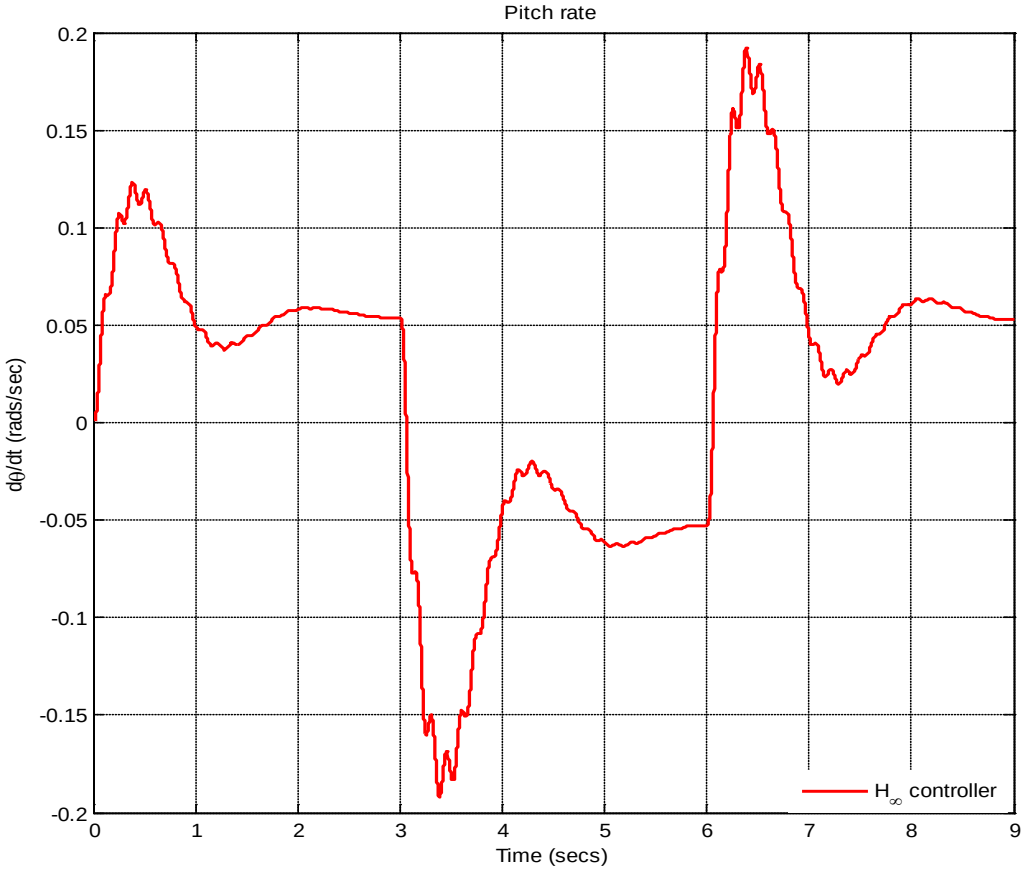

Figure 13. Pitch rate response for H-∞ controller

4.2. H-∞ Loop Shaping Controller Design and Analysis

Here in attitude controller of rocket is designed with n_y and pitch rate as feedback inputs. The pre compensator W_1 selected as

$$W_1 = \begin{bmatrix} W_{11} & 0 \\ 0 & W_{22} \end{bmatrix}$$

where

$$W_{11} = 10\left(\frac{16s + 18}{19s + 2}\right)$$

$$W_{22} = 12\left(\frac{18S + 30}{10S + 8}\right)$$

Pre compensator is always a PI form to have enough slope in the cross frequency while low gain in high frequency can provide enough damping to gain the robustness[17]. The post compensator W_2 is selected as

$$W_2 = \begin{bmatrix} 1 & 0 \\ 0 & 1 \end{bmatrix}$$

where

$$W_{11} = 1 \quad \& \quad W_{22} = 1$$

Post compensator generally reflects the relative importance of outputs to be controlled and therefore it can be chosen as a identity matrix[15]. The diagonal weight function puts constant weights on control actuators[16].In such a way W_1 and W_2 are used to modify the nominal system G as W_2GW_1. The value of ρ is taken as 1.The model matching function is selected as

$$M = \frac{1}{0.0256s^2 + 0.96s + 1}$$

Synthesize the controller K_∞ to make transfer function from disturbance to error minimum. For all MIMO systems for $\gamma < 4$ it can be shown theoretically that controller K_∞ does not change shapes of singular values[19]. The robust stability is achieved without significant degradation in original characteristics. If $\gamma > 4$ then readjust the weight matrix. The controller is synthesized and stability margin (e_{max}) calculated is 0.40851. The gamma value obtained is 2.44792 which satisfies stability margin. Figure 14 shows the frequency response of initial plant and shaped plant.

The sensitivity function of the closed loop system is shown in Figure 15. It can be see that requirement of disturbance attenuation is satisfied[18]. The nominal performance is analyzed and it is 0.0053998 as shown in Figure 16. The frequency response of structured singular values for case of robust stability is shown in Figure 17. The maximum value of μ obtained is 0.25883 which means that stability of closed loop system is preserved under all perturbations that satisfy $\|\Delta\|_\infty < \frac{1}{0.25883}$ [12]. The frequency response of μ for the case of robust performance analysis is given in Figure 18. The peak value of μ is 0.41893 which shows that robust performance is achieved and in higher frequency range it maintains constant value.

Figure 19 shows the transient response of the closed loop system with designed 2 DOF H-∞ loop shaping controller for step signal with magnitude $r = \pm 5$ which corresponds to change in normal acceleration. The overshoot is found to be 14.72%and corresponding settling time is 2.23 sec. The fins deflection obtained is 0.1617 rad. (9.27°) as shown in Figure 20. The pitch rate variation obtained is 0.1 (rad/sec) as shown in Figure 21.

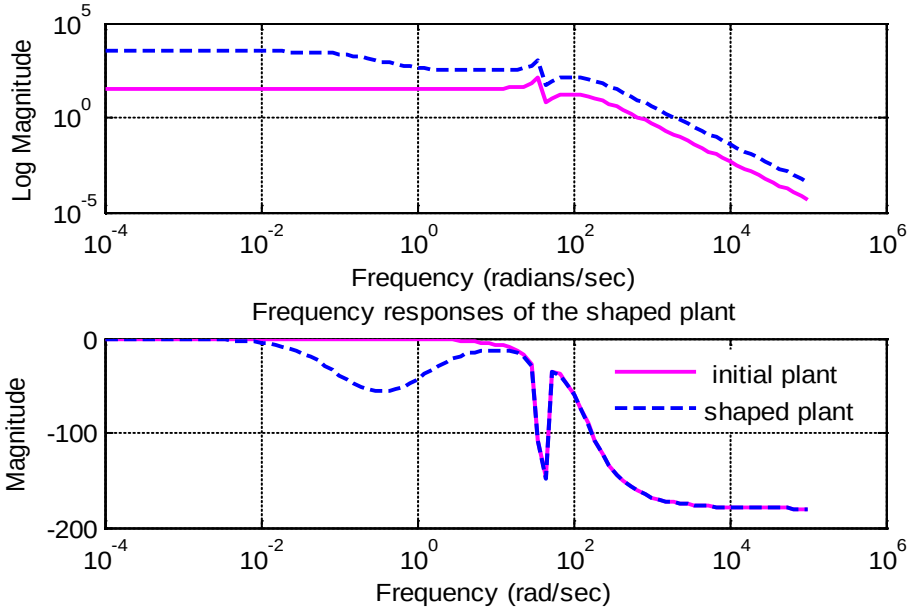

Figure 14. Frequency response of initial plant and shaped plant for H-∞ loop shaping controller

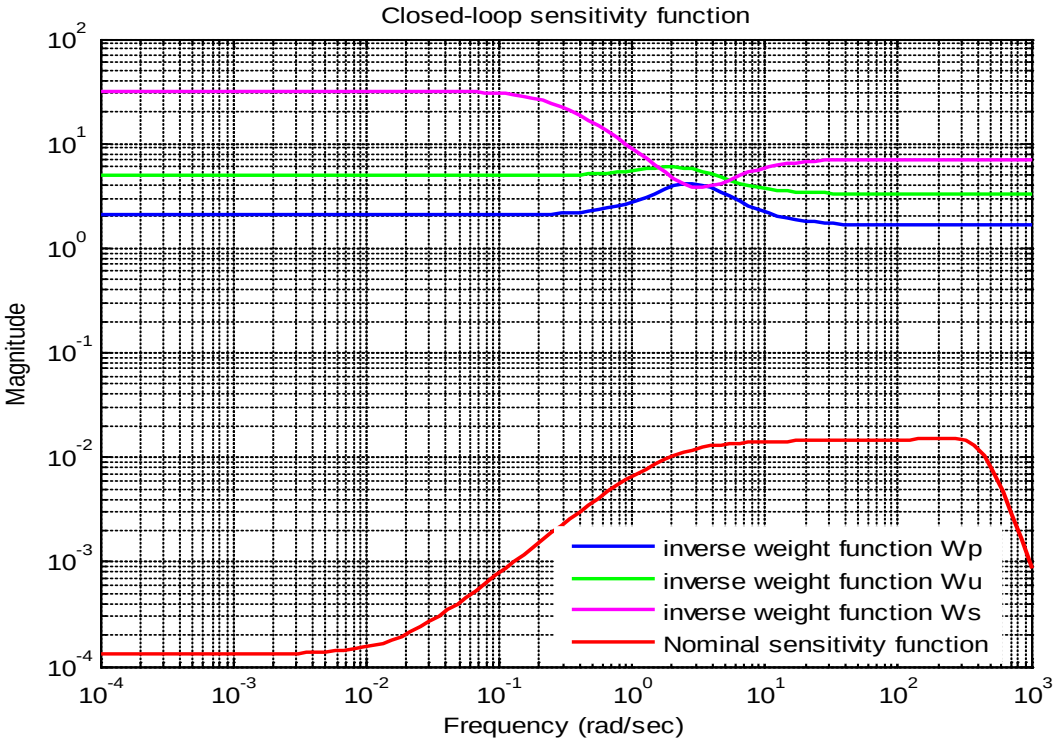

Figure 15. Closed loop sensitivity function for H-∞ loop shaping controller

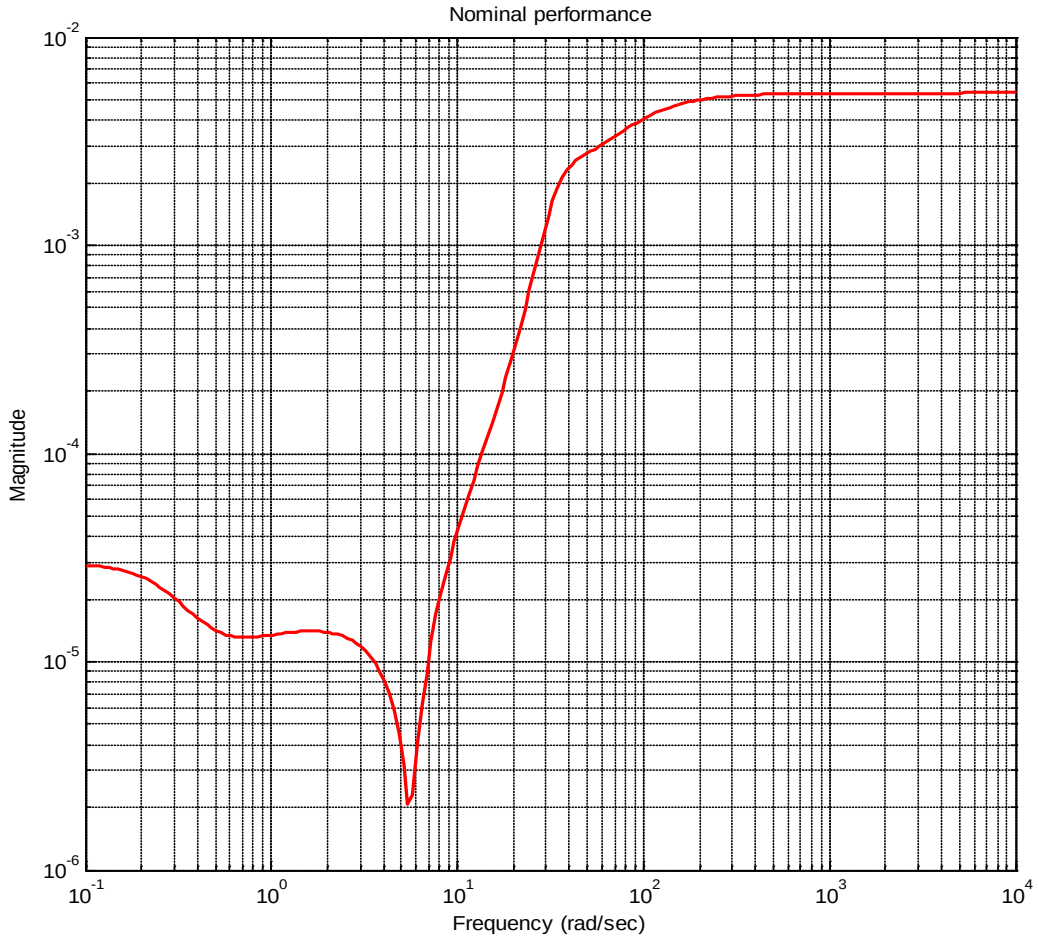

Figure 16. Nominal performance for H-∞ loop shaping controller

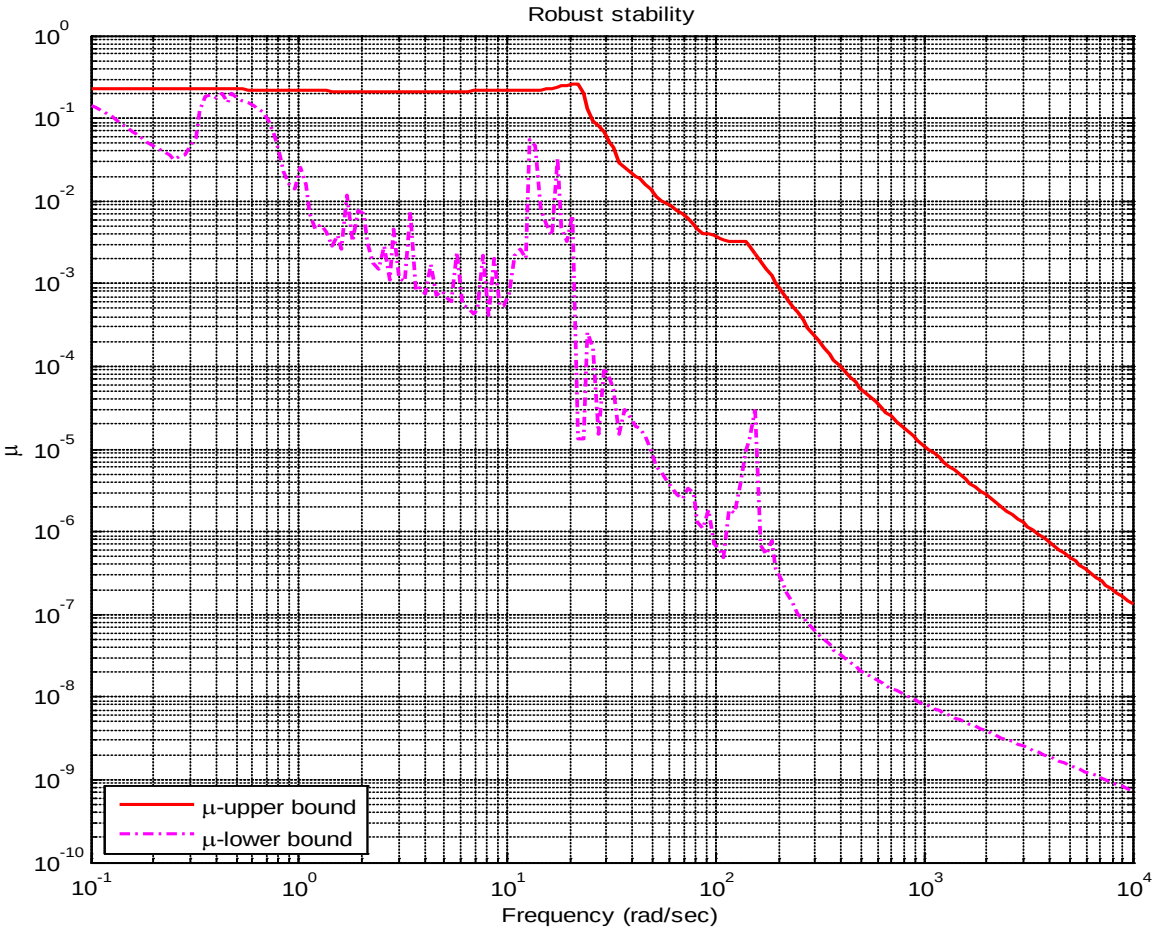

Figure 17. μ- Robust stability for H-∞ controller loop shaping controller

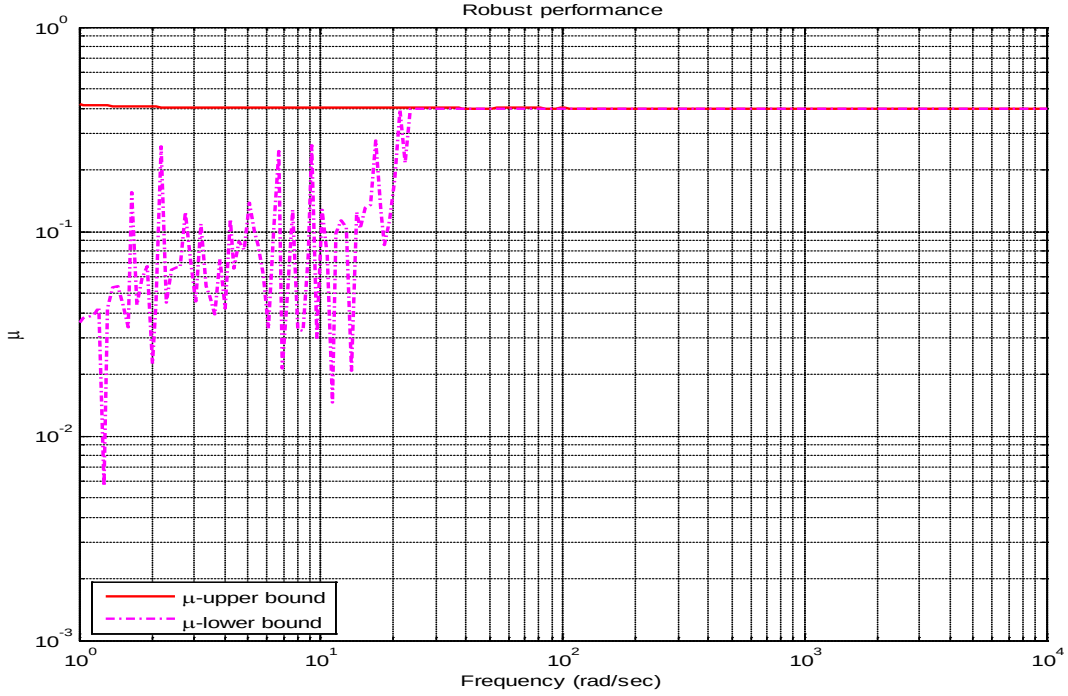

Figure 18. Robust performance for H-∞ loop shaping controller

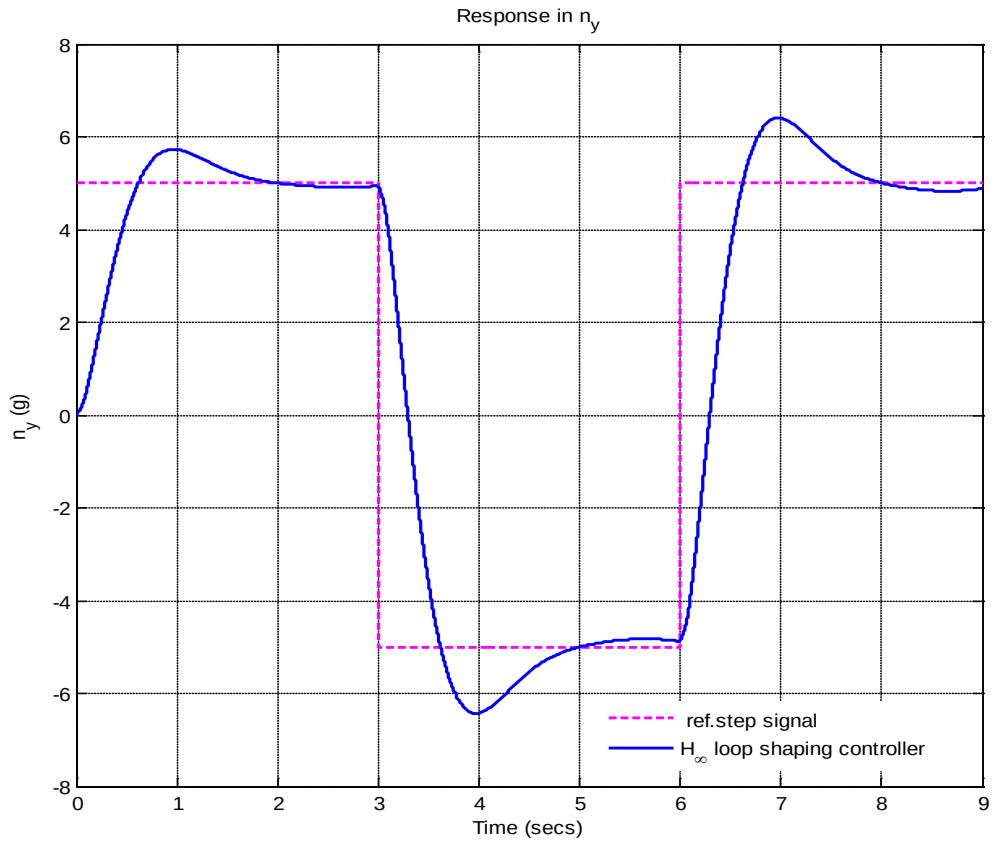

Figure 19. Acceleration response for H-∞ loop shaping controller

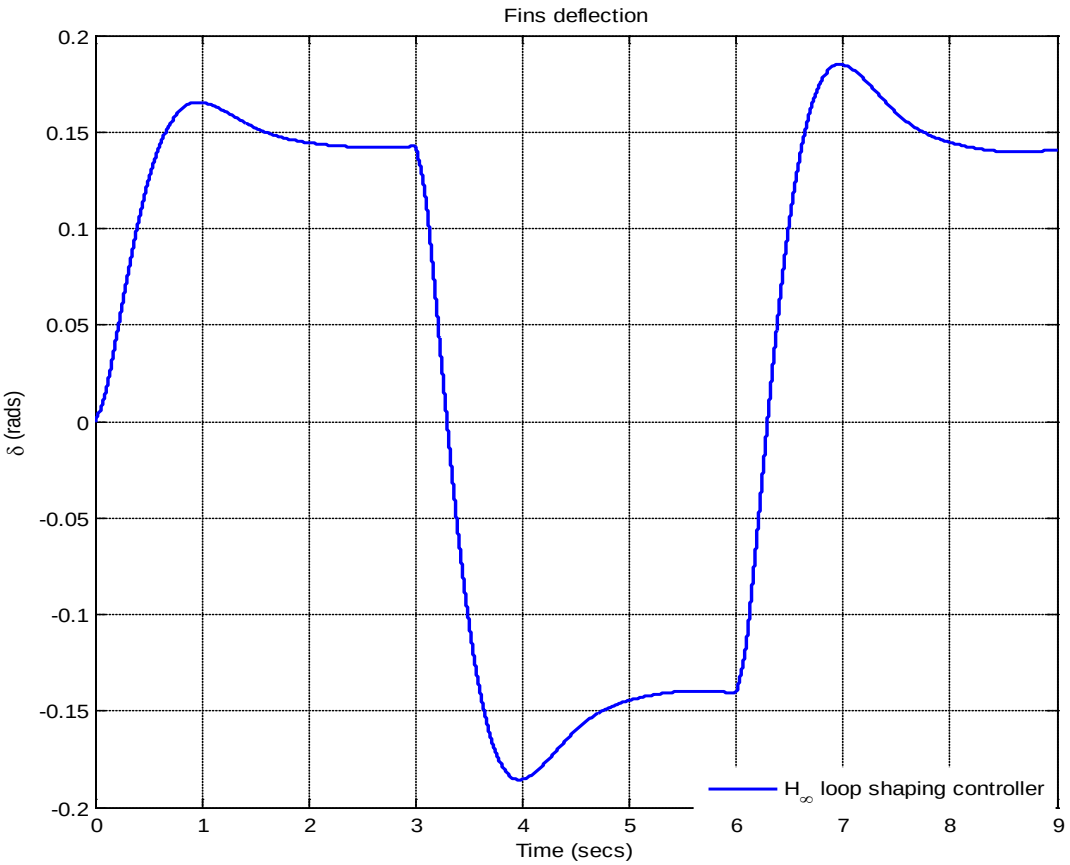

Figure 20. Fins deflection response for H-∞ loop shaping controller

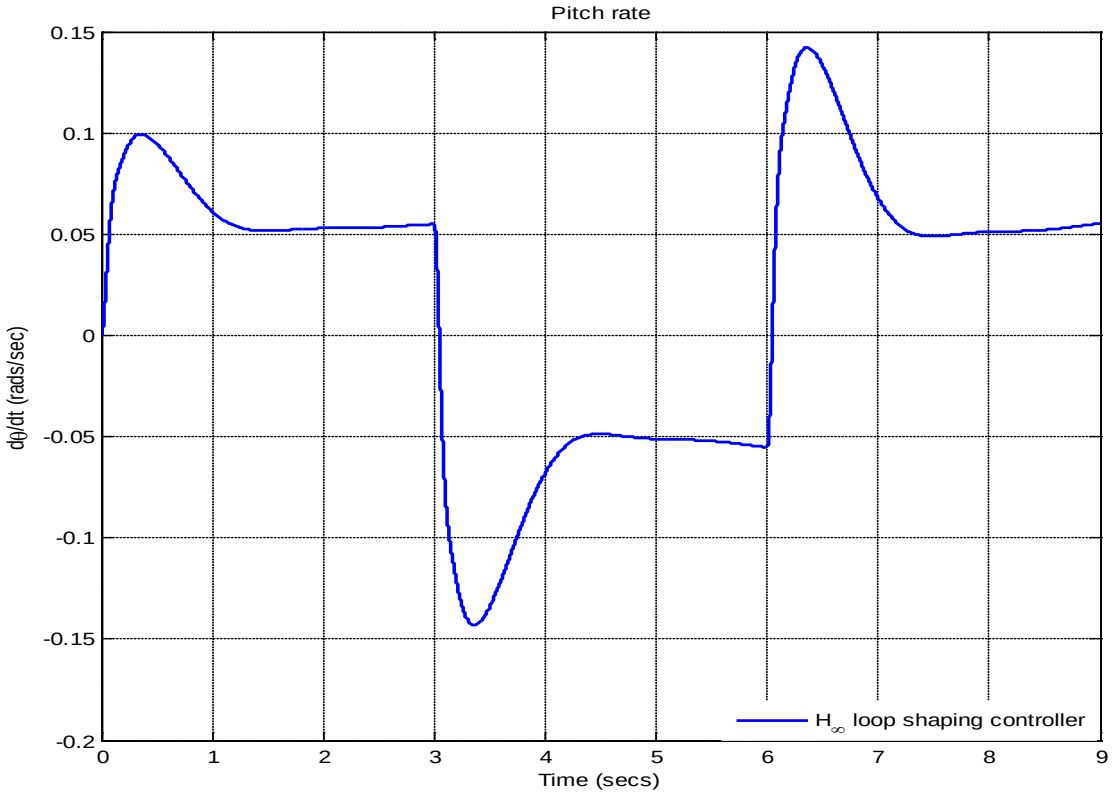

Figure 21. Pitch rate response for H-∞ loop shaping controller

4.3. Comparison and Limitations of Two Approaches

The comparison of closed loop system with H-∞ and H-∞ loop shaping controllers begins with robust stability and performance analysis. To achieve robust stability it is neces sary that the μ values are less than 1 over the frequency range. In Figure 22 we compare the structured singular values, for the robust stability analysis, of the closed-loop systems with both controllers. It shows that H-∞ loop shaping controller achieving better result.

Table 2. Comparison of 2 controllers parameters

parameters	H-∞ controller	H-∞ loop Shaping controller
Nominal performance	0.000398	0.0053998
Robust performance	1.22245	0.41893
μ– robust stability	0.47663	0.25883
Peak overshoot	22.74%	14.72%
Settling time	2.84 Sec	2.23 Sec
Fin deflection	11.78^0 (0.1881 rad)	9.27^0 (0.1617 rad)
RMS value of control signal	0.195587	0.151148

The comparison of nominal performance of two controlle rs is shown in Figure 23. In case of H-∞ loop shaping controller performance is slightly more than H-∞ controller. The slightly larger magnitude over the low frequencies leads to an expectation of steady state errors. The robust performance is also computed as shown in Figure 24. It shows that H-∞ loop shaping controller achieves better performance than H-∞ controller in low frequency range.

The output sensitivity to disturbance is less in H-∞ loop shaping approach as shown in Figure 25. Further we can reduce output sensitivity to disturbance by using high gain values in pre filter design. Transient response of controller is shown in Figure 26. The peak overshoot is reduced in H-∞ loop shaping approach also response is less oscillatory but settling time is not reduced to large extent. As shown in Figure 27 fins deflection is reduced it shows longitudinal stability is improved in H-∞ loop shaping approach. Reduction in pitch rate is also achieved by H- ∞ loop shaping controller as shown in Figure 28. The RMS value of control signal related to fuel consumption. As value decreases proportionally fuel consumption reduced. RMS value is less in H-∞ loop shaping approach so using H-∞ loop shaping controller fuel consumption reduced. Table 2 shows comparison of performance parameters of two controllers.

Figure (22) to (28) shows comparison of parameters of 2 controllers

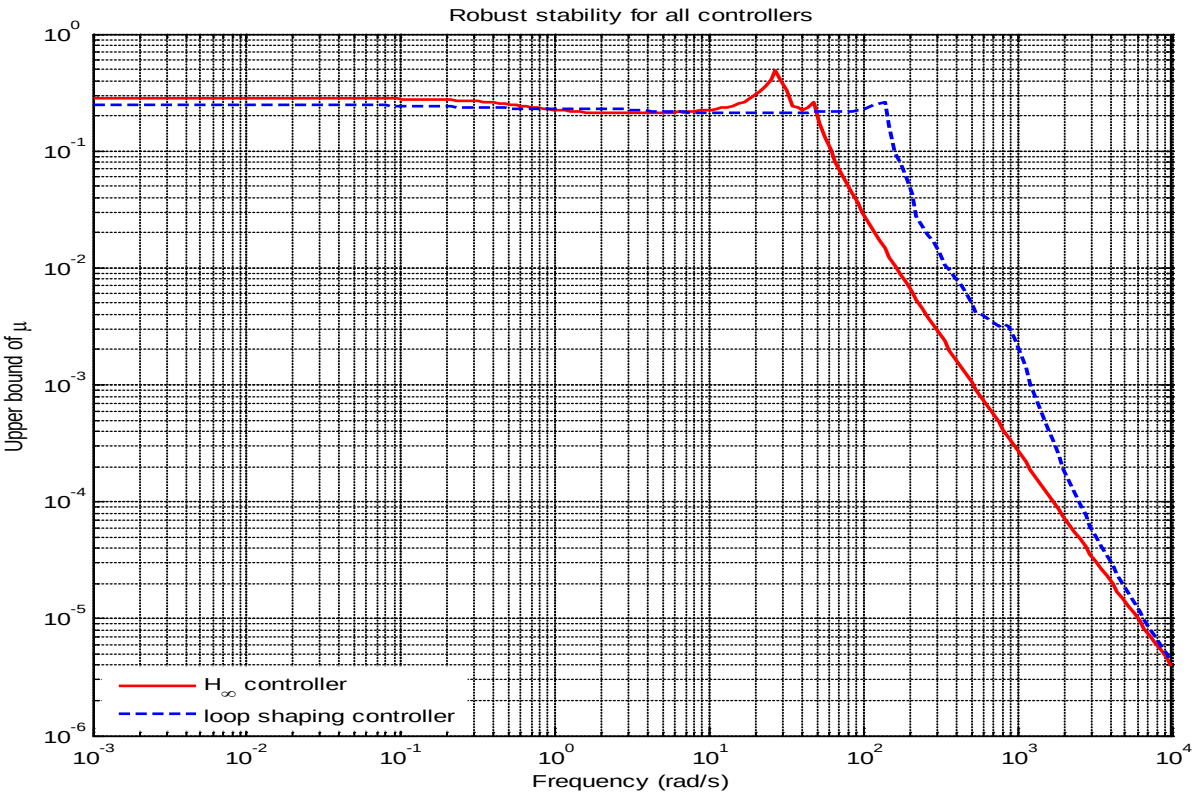

Figure 22. μ- Robust stability for both H-∞ and H-∞ loop shaping controller

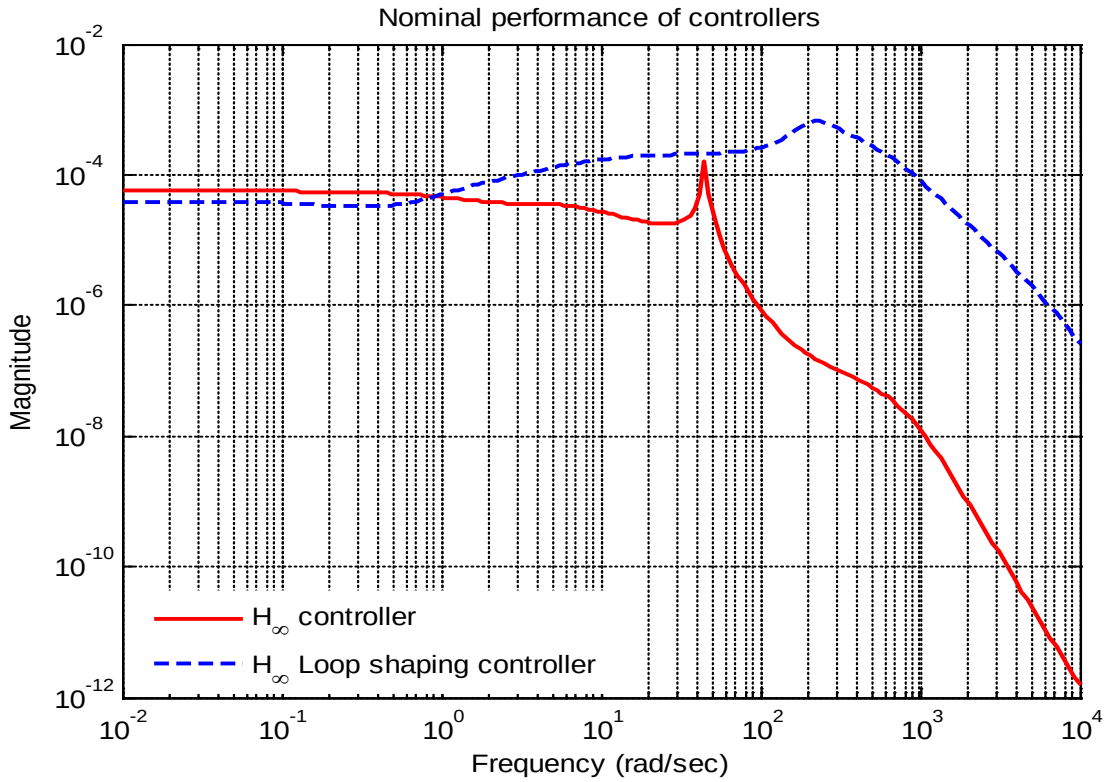

Figure 23. Nominal performance of H-∞ and H-∞ loop shaping controller

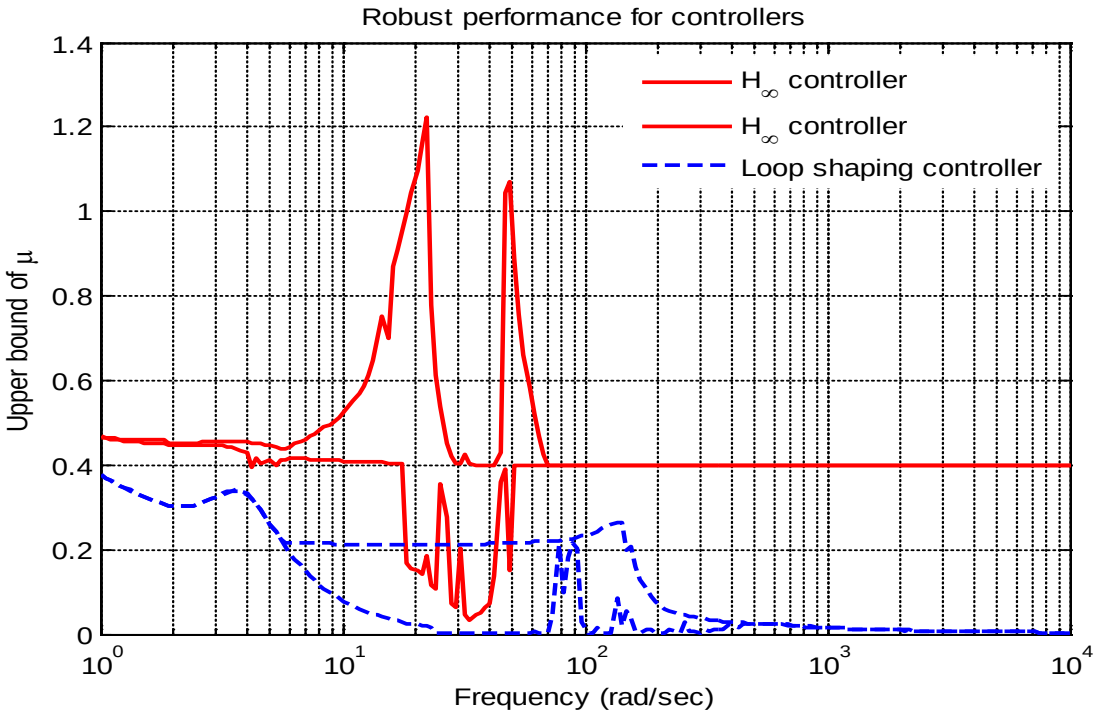

Figure 24. Robust performance for H-∞ and H-∞ loop shaping controller

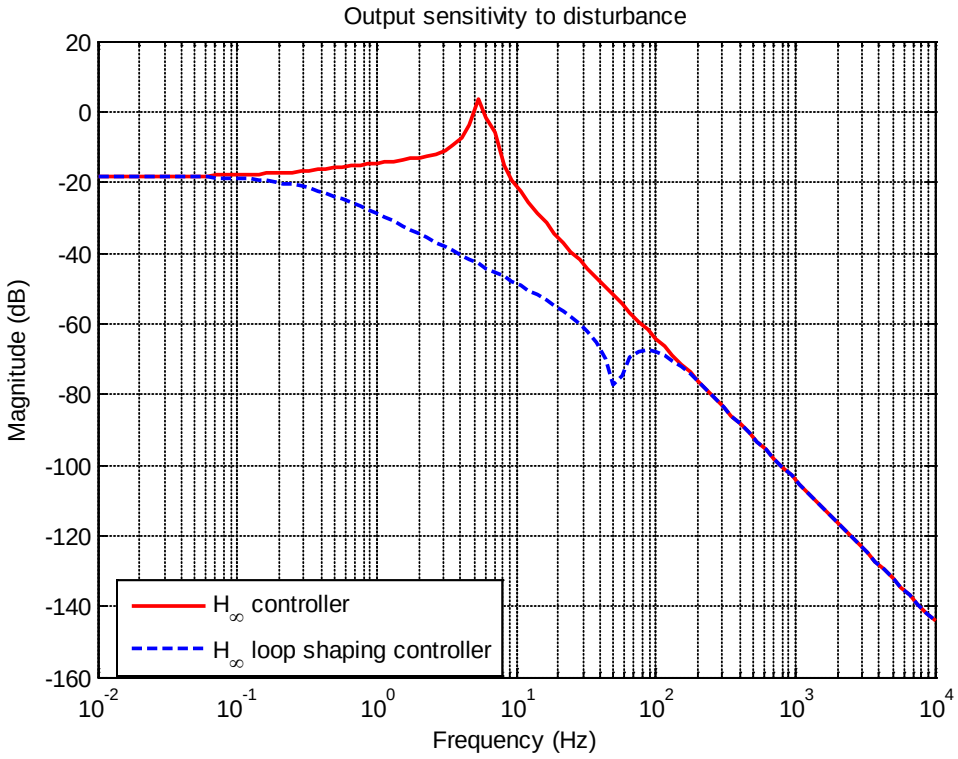

Figure 25. Output sensitivity for H-∞ and H-∞ loop shaping controller

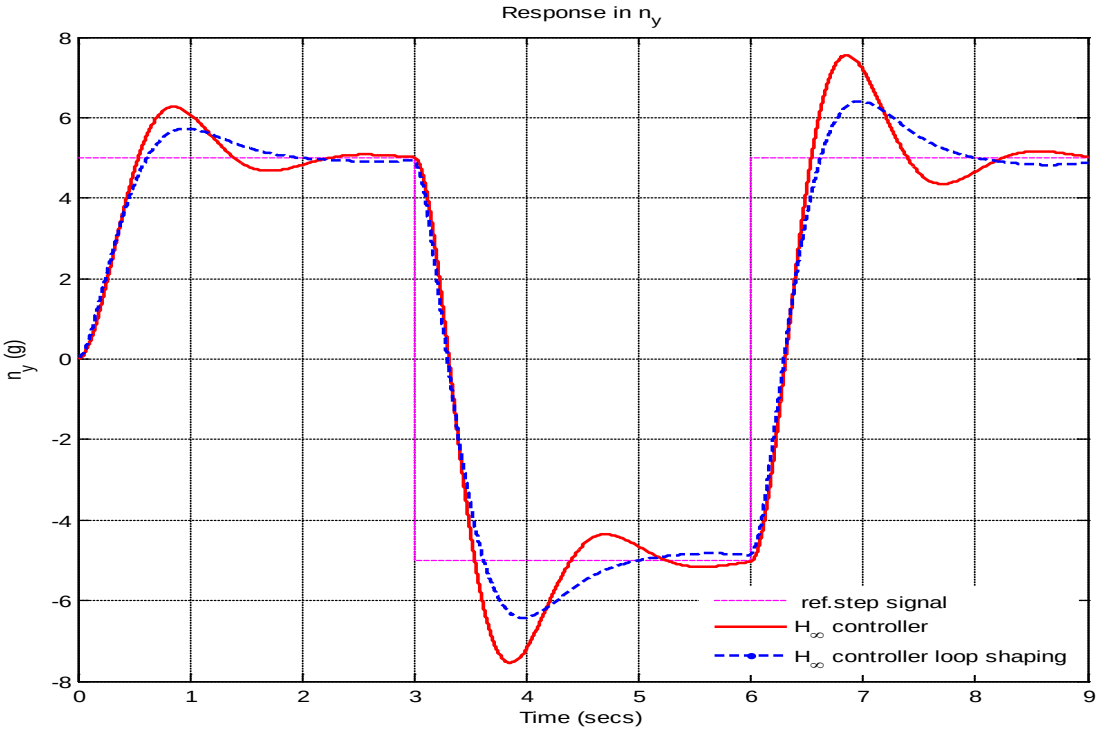

Figure 26. Response for acceleration for H-∞ and H-∞ loop shaping controller

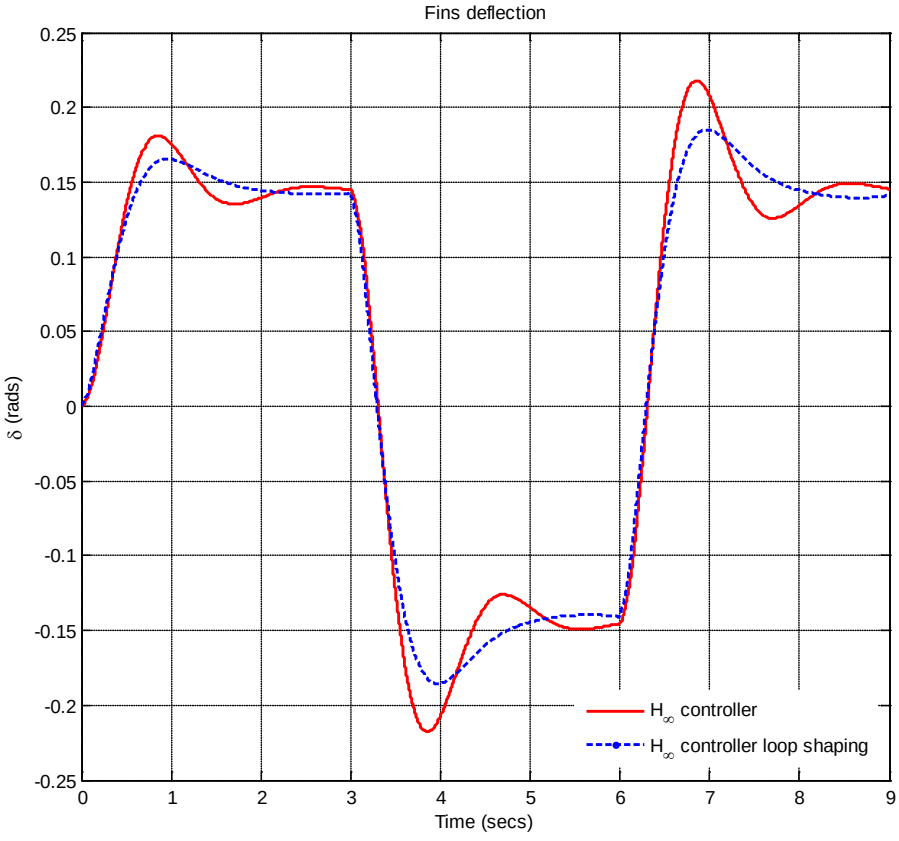

Figure 27. Response for fins deflection for H-∞ and H-∞ loop shaping controller

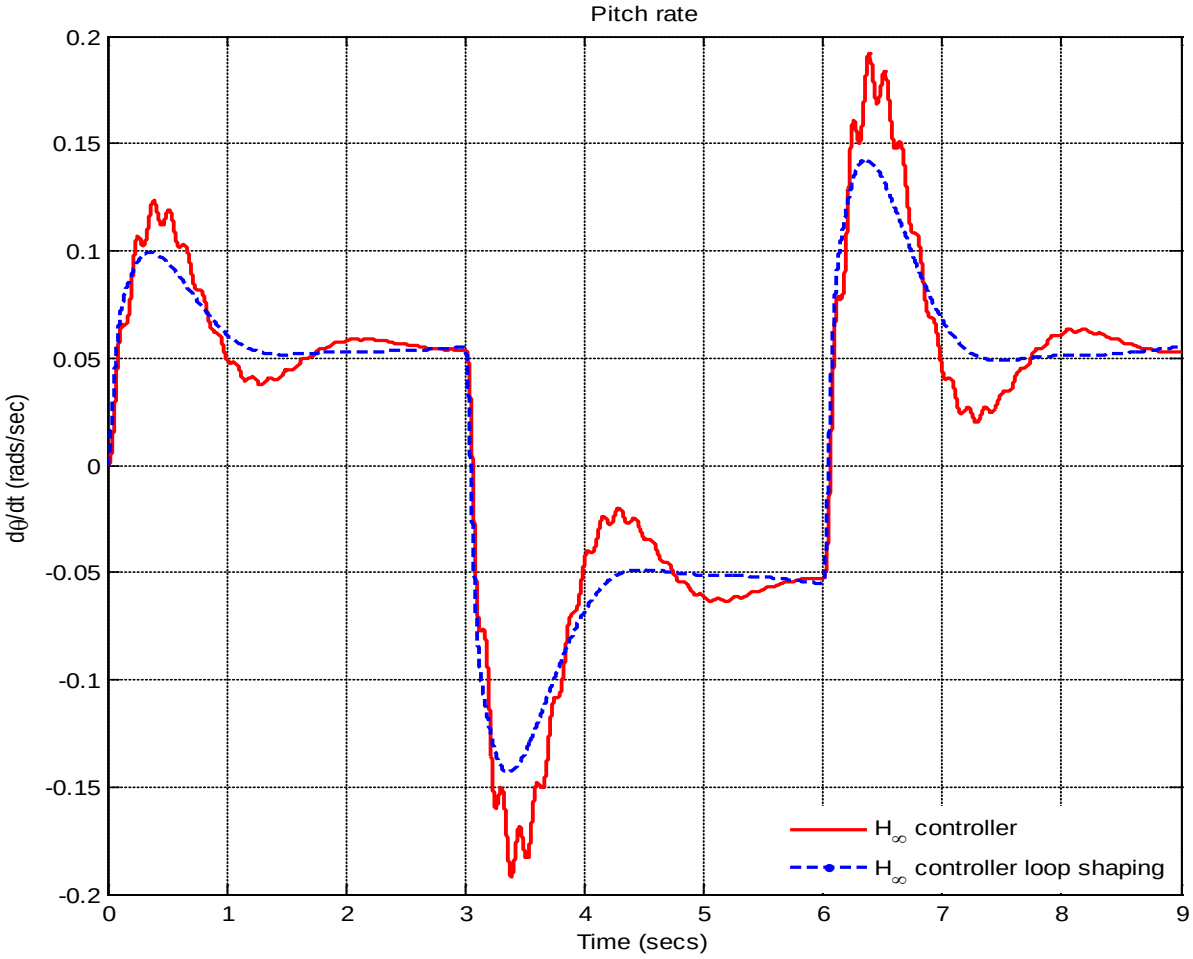

Figure 28. Pitch rate for both H-∞ and H-∞ loop shaping controller

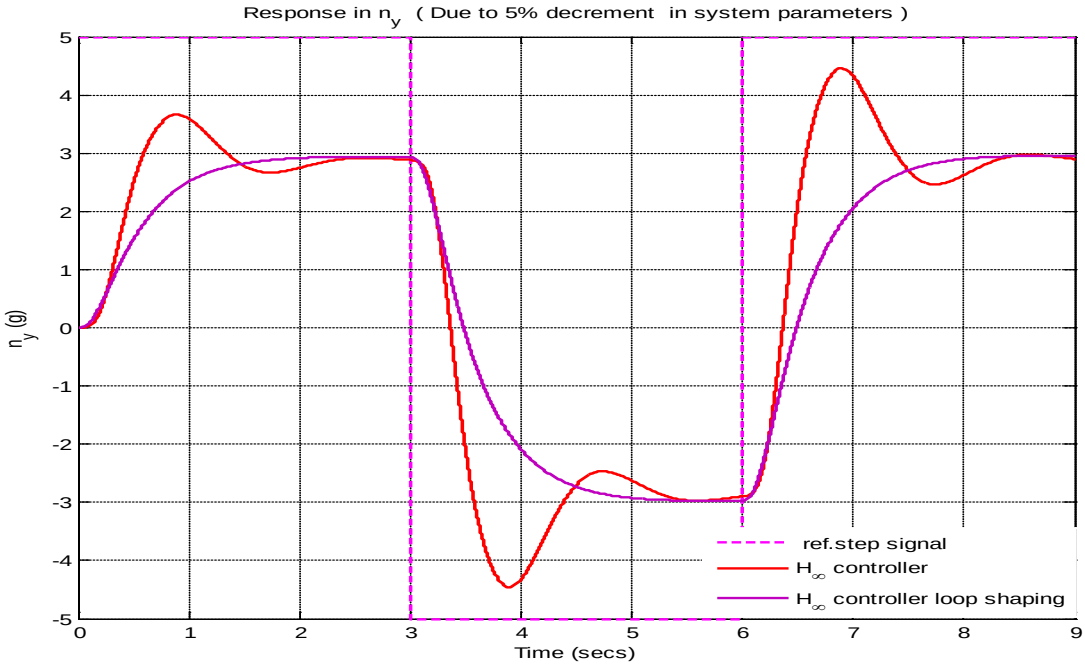

Figure 29. Acceleration response due to 5% decrement parameters

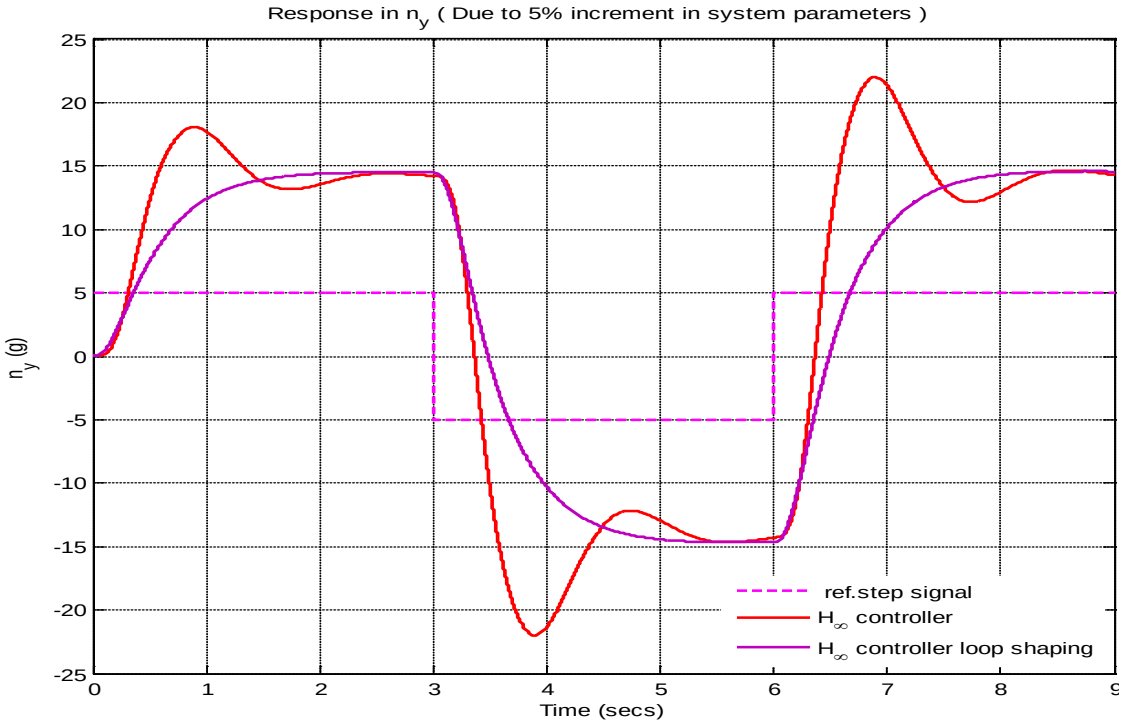

Figure 30. Acceleration response due to 5% increment parameters

In above discussion controllers are designed andcompare d their performance results. Every controller has its specific operating range and depends upon system parameter variati on. In above system 5 % change in system parameters ,the controller fails. Table 3 shows peak over shoot. The responses are shown in Figure 28 and 29.

Table 3. Effect on change in peak overshoot

% change in parameters	Peak overshoot	
	H-∞ controller	H-∞ loop shaping controller
5 % increment	240%	180%
5 % decrement	-196%	-160%

From above table it shows peak overshoot exceeds it maximum limit. So for our controller we can vary system parameters up to 1% obtaining desired value in range .

5. Conclusions

A rocket model is developed in which pitch rate control is analyzed and simulated. The pitch rate control problem is related to the longitudinal stability of the rocket. According to result obtained from simulation it can be seen that longitu dinal stability is improved using 2 DOF loop shaping controller.

Due to presence of uncertain parameters the derivation of the uncertainty model required and heavy computations are demanded. That is the main reason why it is necessary to investigate the parameter importance with respect to the robustness performance and an objective is to reduce their number to an acceptable value. However, in the evaluation of the design, it is better to take into account all the possible uncertainties to ensure a satisfactory design in a present case. Here 15% uncertainties in parameters are taken.

The performance of closed loop system using H-∞ loop controller is evaluated .The model facilitates γ iteration method for solving Ricatti equation for H-∞ controller design The performance of the closed loop systemusing H-∞ loop shaping controller is further evaluated. The application of a 2 DOF H- ∞ loop shaping controller in pitch rate auto pilot design shows that it is better in robustness and reduces control efforts without the degrading performance.

Actuator efforts are critical consideration in the rocket auto pilot design since they invoke how quickly actuator command limiting is invoked. The pitch rate reduced and reduction in fins deflection shows that actuator efforts are reduced.

Nomenclature

Symbol	Meaning
ϑ	Pitch Angle
ψ	Yaw Angle
γ	Roll Angle
α	Angle Of Attack
β	Sideslip Angle
Θ	Flight-Path Angle
Ψ	Bank Angle
γ_c	Aerodynamic Angle Of Roll
$\delta_{y,}\delta_z$	Angles DueTo Fins Deflection In Longitudinal And Lateral Motion
M	Mach Number

REFERENCES

[1] Zames G.(1981) "Feedback and optimal sensitivity model reference transformation, multiplicative semi norms and approximate references." *IEEE Transaction On Automatic Control* AC-23 (1981), 301-302

[2] Doyle J., Glover K, Khargoeker P., and Fracis B (1989) "State space solution to standard H_2 and H_∞ control problem" *IEEE Transaction On Automatic Control* 34 (1989), 831-847

[3] Glover k, Limebeer D, Doyle j, Kasenally E.M, and Sofonov M, (1991) "A characterization of all solutions to four block distance problem" *SIAM Journal of control and optimization* , 29 (1991) 283-324

[4] Reichert R T (1989) "Application of H_∞ control to missile autopilot design" In *Proceedings Of AIAA Guidance , Navigation And Control Conference* , 1989 1065-1072

[5] McFarlane, D.C., and K. Glover, "A Loop Shaping Design Procedure using Synthesis," IEEE Transactions on Automatic Control, vol. 37, no. 6, pp. 759– 769, June 1992.

[6] George m. Siouris "Modern missile guidance and control" springer – verlag .2004 (e-book)

[7] Brodsky, S.A.; Aro, H.O (2011) "Application of robust control for attitude stabilization of supersonic winged rocket" *IEEE Transaction On Control System*, 978 – 1 – 4244 – 9616 - 7/11,2011

[8] J.Blaklock " *Automatic control of Aircraft & missiles "*. John wiley & sons. 2004

[9] Jack E. Nelsen "Missile Aerodynamics" *Mc Graw Hill Publications* 1960

[10] D.W.Gu , P. Peter "Robust control engineering design with MATLAB" .*springer – verlag*, 2005 1st Edition

[11] S.Skogested, I.Postlethwaite "Multivariable feedback control system *" wiley & sons* .2001

[12] M Green "Linear robust control" chapter 6: Full information about H-∞ synthesis. *Dover publication* .1998

[13] Mark .R. Tucker.and Daniel Walker." H-∞ mixed sensitivity ", *Robust flight control- Design challenge, leacture notes in control and information science*, Springer- Verlag 2000

[14] Yang S M and Huang H " Application of H-∞ control to missile auto pilot design" *IEEE transaction on Control system* 0018-9251/03

[15] R. Sobhani " Nonlinear Digital Robust controller for UAV", *IEEE Aerospace conference* 1-4144-0525-4/2007

[16] Sun Jie, Yang Jun " Robust flight control law development for Tiltrotor conversion" *IEEE 2009 International conference on intelligent human machine system and cybernetics* 978/0-7695-3753-8/09

[17] Mingyun L V, Yanpenh Hu" Attitude control of unmanned helicopter using H-∞ loop shaping method" *IEEE Transaction on Mechatronics sciences* 978 – 1 – 61284 – 722 - 1/11 ,2011

[18] J.Gadewadikar, F.L.Lewis, Kamesh Subbarao and Ben M. Chen. "Structured H∞ Command and Control-Loop Design for Unmanned UAV". *Journal Of Guidance, Control, And Dynamics. Vol. 31. No. 4, July-August* 2009.

[19] J. Gadewadikar, F. L. Lewis, Kamesh Subbarao and Ben M.Chen.Attitude "Control System Design for Unmanned Aerial Vehicles using H-∞ and Loop-shaping Methods." *2007 IEEE International Conference on Control and Automation. Guangzhou, CHINA* May 30 to June 1,2007.

[20] K Glover and R Hyde "H-∞ Loop shaping design for Flight", Chapter 29 Robust flight control- Design challenge, lecture notes in control and information science, *Springer- Verlag* 2000

[21] T Chelaru, C Barbu " mathematical model and technical solution for multistage sounding rocket" *IEEE proceedings on international conference on applied mathematics and simulation, modeling 2009*,978-960-474-147-2/0.9